

A new chronostratigraphy (^{40}Ar - ^{39}Ar and U-Pb dating) for the middle section of the Burdur-Fethiye Shear Zone, SW Turkey (eastern Mediterranean)

İrem ELİTEZ^{*} , Cenk YALTIRAK , Gürsel SUNAL 

Department of Geological Engineering, Faculty of Mines, İstanbul Technical University, İstanbul, Turkey

Received: 12.03.2018 • Accepted/Published Online: 17.07.2018 • Final Version: 28.09.2018

Abstract: Southwestern Turkey is a tectonically active region where extensional, strike-slip, and compressional tectonics cooccur. The Burdur-Fethiye Shear Zone is located in the middle of this complex area. Understanding the tectonic evolution of this region is crucial, but the controversial Neogene chronostratigraphy does not allow robust synthesis because of poor age control. The middle section of the Burdur-Fethiye Shear Zone includes three basins: the Acıpayam, Çameli, and Gölhisar basins. All these basins represent restricted portions of ancient larger carbonate lakes. The lacustrine sediments are locally covered or cut by lamproites with sparse intercalations of tuff levels. New ^{40}Ar - ^{39}Ar biotite and U-Pb zircon radiometric ages from volcanics and a tuff layer in this study demonstrate that the previously suggested Pliocene ages for these sediments are incorrect and that these Neogene sediments are middle Miocene in age.

Key words: ^{40}Ar - ^{39}Ar biotite dating, U-Pb zircon dating, Neogene stratigraphy, Burdur-Fethiye Shear Zone, Acıpayam Basin, Çameli Basin, SW Turkey

1. Introduction

Southwestern Turkey is a tectonically complex and active region in the Anatolian Microplate. Various hypotheses have been proposed for the tectonic evolution of this region, where structures formed associated with: 1) the westward escape of the Anatolian Microplate (Dewey and Şengör, 1979; Şengör, 1979; Şengör et al., 1985); 2) the NE-SW back-arc extension of the Aegean region (McKenzie, 1978; Le Pichon and Angelier, 1979; Meulenkamp et al., 1988; Yılmaz et al., 2000); 3) the subduction-transform edge propagator fault zone related to the motion of the Hellenic and Cyprus arcs (Govers and Wortel, 2005; Hall et al., 2014a); and 4) the compressional region of the Western Taurides (Aksu et al., 2009, 2014; Hall et al., 2009, 2014a, 2014b). The Burdur-Fethiye Shear Zone is a transtensional left-lateral shear zone 75–90 km wide and 300 km long, located along the southeastern boundary of the large Aegean extensional region and forming the western part of the Isparta Angle (Figure 1; Hall et al., 2014a; Elitez et al., 2016). The middle section of this shear zone consists of an ancient basin fill including the middle Miocene to lower Pliocene sequence, accumulated in fluvial and lacustrine environments and deformed by left-lateral transtensional shearing (Elitez et al., 2016; Elitez and Yaltırak, 2016). Today this region includes the Acıpayam, Çameli, and Gölhisar basins and their modern basin fill consisting of

Pliocene–Quaternary units (Elitez and Yaltırak, 2016). In most previous studies the local fluvial, lacustrine, and alluvial fan deposits were mapped together and assigned a Pliocene age (e.g., Şenel, 1997, 2002). Such terrestrial sediments were first named the Çameli Formation (Erakman et al., 1982), but were subsequently divided into three members: the basal alluvial-fan Derindere Member, the middle fluvial Kumavşarı Member, and the upper lacustrine Değne Member (Alçıçek et al., 2004, 2005, 2006). Later, Elitez and Yaltırak (2014, 2016) mapped these three sediment successions as the Gölhisar, İbecik, and Dirmil formations. Based on micromammal fauna, the lacustrine sediments of the İbecik Formation were assigned an age of 10.8–8.5 Ma (Saraç, 2003) or ~3.4 Ma (van den Hoek Ostende et al., 2015b), while the upper section of the sedimentary sequence was dated as 1.8–2.2 Ma (e.g., Alçıçek et al., 2005, 2006; van den Hoek Ostende et al., 2015a). Recent studies showed that this significant time gap caused the development of an angular unconformity between lacustrine and alluvial fan sediments (Elitez and Yaltırak, 2016; Elitez et al., 2016). In the northern part of the study area, there are volcanic rocks that cut and/or overlie the lacustrine sediments. A small number of ^{40}Ar / ^{39}Ar radiometric dates from these volcanic rocks were obtained by Paton (1992) and reported ages range between Tortonian and early Pliocene. Further, however,

* Correspondence: elitezi@itu.edu.tr

these sediments were assigned to the middle Miocene-upper Pliocene based on previously dated volcanic rocks, reliable micromammal fossil records, and stratigraphic relationships (Elitez and Yaltrak, 2014, 2016).

The above review of the existing literature shows that the chronostratigraphy of the Acıpayam, Çameli, and Gölhisar basins and their environs is controversial. The chronostratigraphy of these basins remains one of the most important problems in the region because of its vital role in the tectonic and kinematic history of southwestern Anatolia, including the Burdur-Fethiye Shear Zone. The data we obtain can redefine all the events along the Burdur-Fethiye Shear Zone. Based on the ages of these sediments, the timing of tectonic events both in western and southwestern Anatolia will be modified and the

geological construction of the region will be reinterpreted. In an attempt to resolve the conflicting chronostratigraphic interpretation of the Neogene successions across the Acıpayam, Çameli, and Gölhisar basins and environs, we collected seven volcanics and a tuff sample for radiometric dating. U-Pb zircon and ^{40}Ar - ^{39}Ar biotite methods were applied on the samples and the results show that lacustrine sediments are upper Miocene in age rather than Pliocene.

2. Description of local stratigraphic units

2.1. Basement rocks

The Neogene Acıpayam, Çameli, and Gölhisar basins developed over Paleozoic to early Miocene basement rocks. These basement rocks are composed of Lycian nappes (Brunn et al., 1970; Graciansky, 1972; Önalın,

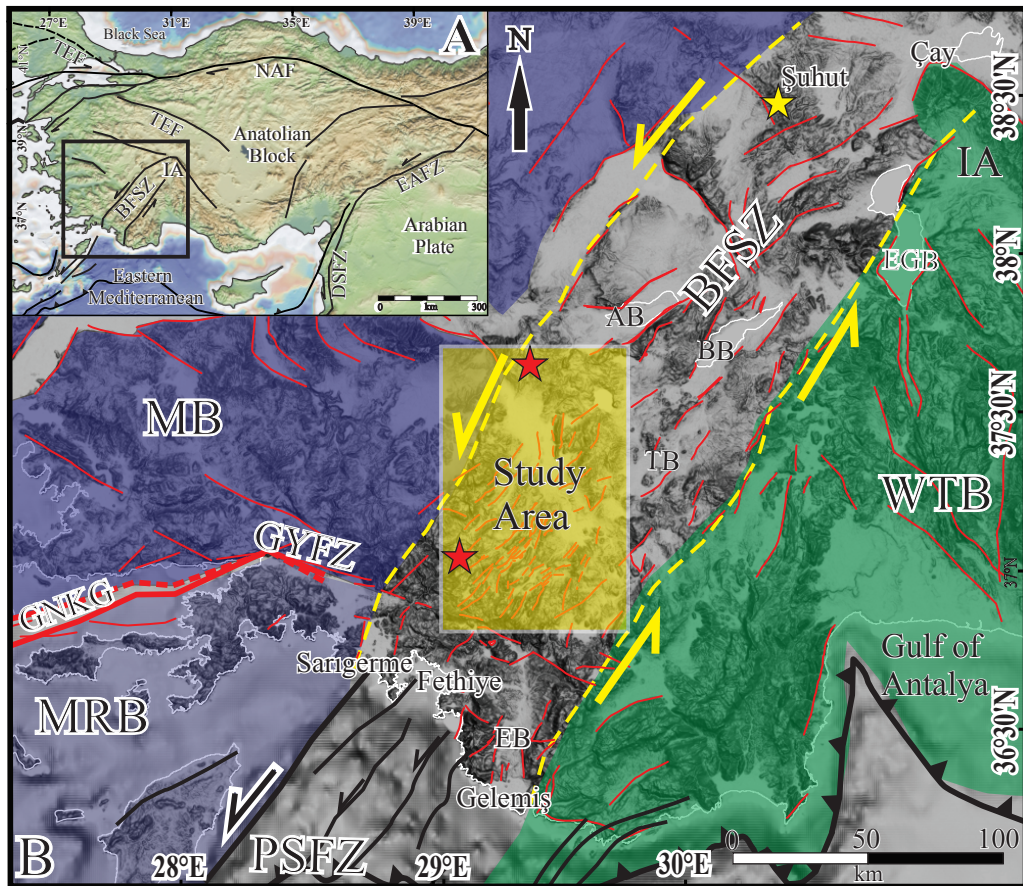


Figure 1. A) Simplified neotectonic map of Turkey compiled from Yaltrak et al. (2012). TEF: Thrace-Eskişehir Fault, NAF: North Anatolian Fault Zone, EAFZ: East Anatolian Fault Zone, DSFZ: Dead Sea Fault Zone, IA: Isparta Angle, BFSZ: Burdur-Fethiye Shear Zone. Rectangle indicates Figure 1B. B) Regional fault map of southwestern Anatolia compiled from Tur et al. (2015). Yellow rectangle indicates location of the study area. Dark blue region denotes the NE-SW extensional domain. (MRB: Marmaris-Rhodes Block, MB: Menderes Block, GNKG: Gökova-Nisyros-Karpathos Graben). Green region denotes the NNE-SSW compressional domain (WTB: Western Taurides Block, IA: Isparta Angle). BFSZ: Burdur-Fethiye Shear Zone, PSFZ: Pliny-Strabo Fault Zone, GYFZ: Gökova-Yeşilüzümlü Fault Zone, AB: Acıgöl Basin, BB: Burdur Basin, TB: Tefenni Basin, EGB: Eğirdir Basin, EB: Eşen Basin. Red stars indicate locations of dated samples in this study. Yellow star indicates location of dated samples of Prelević et al. (2015).

1979; Ersoy, 1990) and Yeşilbarak nappe (Önalın, 1979) and consist of Paleozoic rocks, Mesozoic volcanic rocks, Mesozoic sedimentary rocks, Mesozoic limestones, Cretaceous ophiolitic mlange, Cretaceous flysch, Paleogene sedimentary rocks, and Eocene-lower Miocene turbiditic sedimentary rocks. The Paleozoic rocks comprising limestones, dolomites, radiolarites, cherts, shales, and sandstones (Şenel, 1997) are generally exposed in the southwestern part of the study area (Figure 2). The Mesozoic volcanic rocks, including basalts, spilitic basalts, and rarely radiolarites, cherts, and shales (Şenel, 1997), crop out on the southwestern side of the study area. The Mesozoic sedimentary rocks consist of sandstones, mudstones, and conglomerates and can be observed in two small areas in the northwestern and southwestern parts of the study area. The Mesozoic limestones, composed of locally recrystallized pelagic and neritic limestones, generally cover topographically high areas (Figure 2). The Cretaceous ophiolitic mlange mainly comprises harzburgites, serpentinites, dunites, and radiolarites and covers an extensive area (Figure 2). The Cretaceous flysch is turbiditic in nature and is characterized by sandstones, claystones, cherty limestones, and conglomerates (Şenel, 1997). These rocks outcrop as small exposures in the study area (Figure 2). The Paleogene sedimentary rocks include conglomerates, sandstones, siltstones, and shales and are exposed on the western and northwestern parts of the study area. The Eocene-lower Miocene turbiditic sediments consist of sandstones, claystones, siltstones, shales, and mudstones.

2.2. Bozdağ Formation

The Neogene basin fills start with alternating conglomerates, sandstones, and mudstones of the Bozdağ Formation (Gktaş et al., 1989). The Bozdağ Formation unconformably overlies the basement rocks and is unconformably overlain by the Glhisar Formation (Figure 2). The best exposures of the unit are located in the northern portion of the study area, northeast of Kelekçi and in the valley between the villages of Ören and Mevltler (Figure 2 and 3). The Bozdağ Formation consists of medium to thick-bedded, locally massive, dark-gray, gray, light-brown, yellowish, and reddish conglomerates, sandstones, and mudstones. It is approximately 500 m thick. Based on its stratigraphic position and algae fossils such as *Schizotrix* sp. and *Scytonema* sp., Şenel (1997) dated the formation as upper Oligocene-lower Miocene. The Bozdağ Formation contains sedimentary facies representing a coastal environment under terrestrial influence.

2.3. Glhisar Formation

The Glhisar Formation contains green, greenish gray-to-gray, reddish brown, brown, and purple conglomerates and sandstones. This unit was identified by Elitez (2010).

The best outcrops and cross-sections are observed north of Glhisar, south of Acipayam, and along the new Acipayam-Çameli main road (Figure 2). The Glhisar Formation unconformably or occasionally tectonically rests on the basement rocks and grades vertically and horizontally into the İbecik Formation (Figure 3). The succession starts with thick beds of granule conglomerates at the bottom and grades upward into conglomerates, conglomeratic sandstones, sandstones, and siltstones. The pebble composition of conglomerates varies depending on the characteristics of the local basement rocks (e.g., serpentinite, radiolarite, and limestone pebbles). However, around Acipayam and north of Yeşilyuva, the pebbles are composed primarily of reworked material derived from the Bozdağ Formation.

The thickness of the unit is ~900 m. Lack of fossil data does not allow a proper dating. Therefore, the age of the formation is thought to be middle-late Miocene due to its stratigraphic position (Elitez, 2010; Elitez and Yaltırak, 2014, 2016). The Glhisar Formation was deposited in a meandering and/or braided river system. The limestone lenses at the bottom of the unit indicate a reefal environment near Acipayam and northern of Yeşilova.

2.4. İbecik Formation

The İbecik Formation (Elitez, 2010) is predominantly composed of white, beige, and yellowish sandstones, siltstones, claystones, marls, tuffs, and limestones. The best cross-sections are observed near the village of İbecik, along the NE-SW road from the Yapraklı dam to a small hill to the northeast (Figure 2). The İbecik Formation grades laterally and vertically into the Glhisar Formation at the bottom and is unconformably overlain by the Dirmil Formation. The succession starts with beige sandstones and whitish gray claystones that grade upwards into white and grayish fractured marls and limestones. The uppermost part of the İbecik Formation includes mostly red wine-colored claystones and hard, locally fractured, thickly bedded, whitish yellow and red wine-colored silty carbonates including caliche. The thickness of this upper part is ~200 m and it records a period of aridity. There are intercalating vertical transition with tuffs rich in biotite. Especially in the southernmost part of the study area, biotites of 2–3 mm in size are observed. They are commonly found among the marl levels of the İbecik Formation. The İbecik Formation is ~850 m thick. In the northern part of the study area, the sediments of the İbecik Formation are covered or cut by Denizli lamproites (Paton, 1992) at elevations of 1300–1600 m (Figures 2 and 3).

Based on vertebrate fossils at 1400 m elevation south of the village of Elmalıyurt (36°53'18.34"N, 29°21'33.73"E), the marls and thin coal beds of the İbecik Formation are assigned a Vallesian age (Saraç, 2003). The evolutionary stages of the lacustrine deposits indicate a continuous

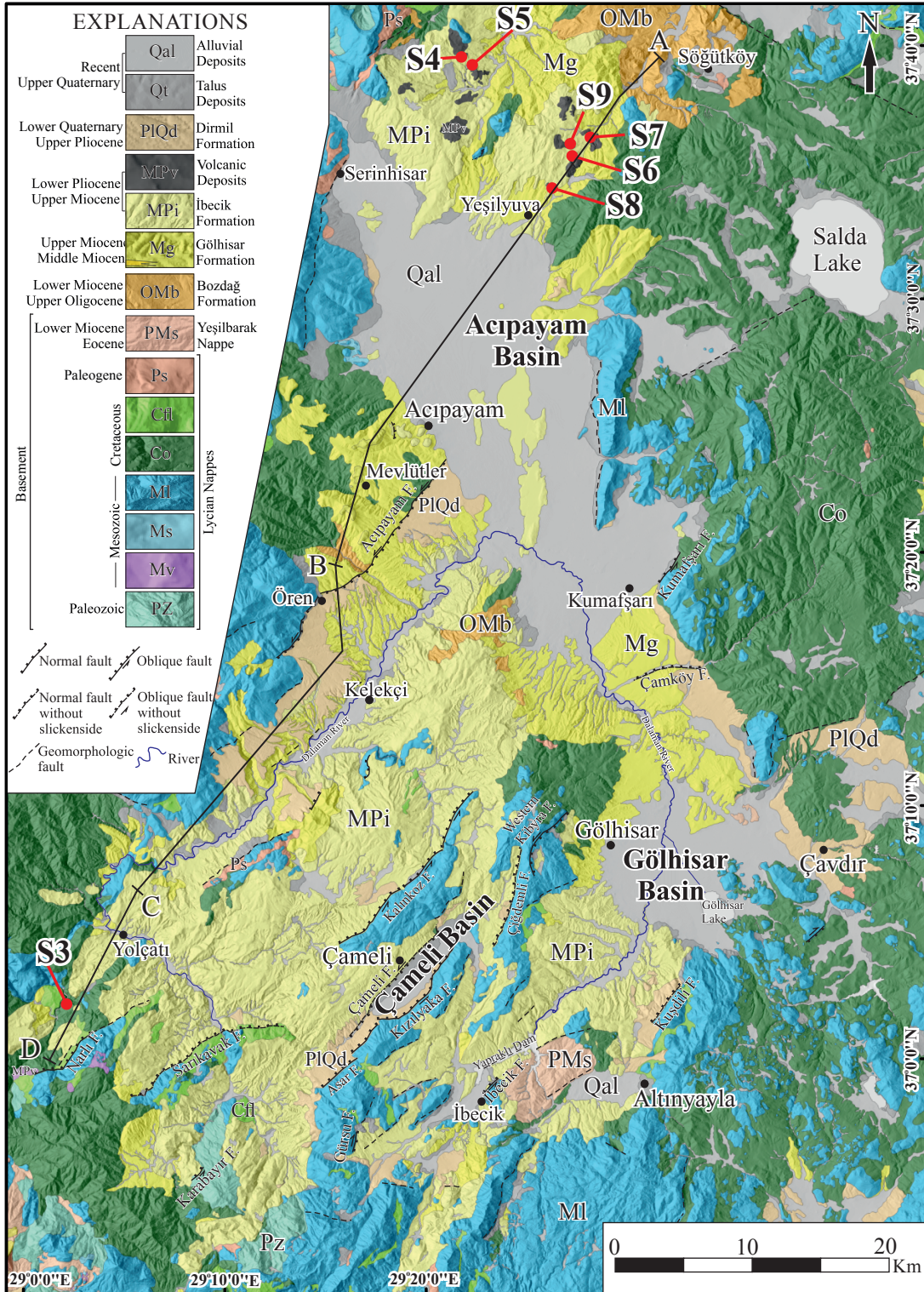


Figure 2. Simplified geological map of the study area (Elitez and Yaltrak, 2016). Red points show the locations of the samples.

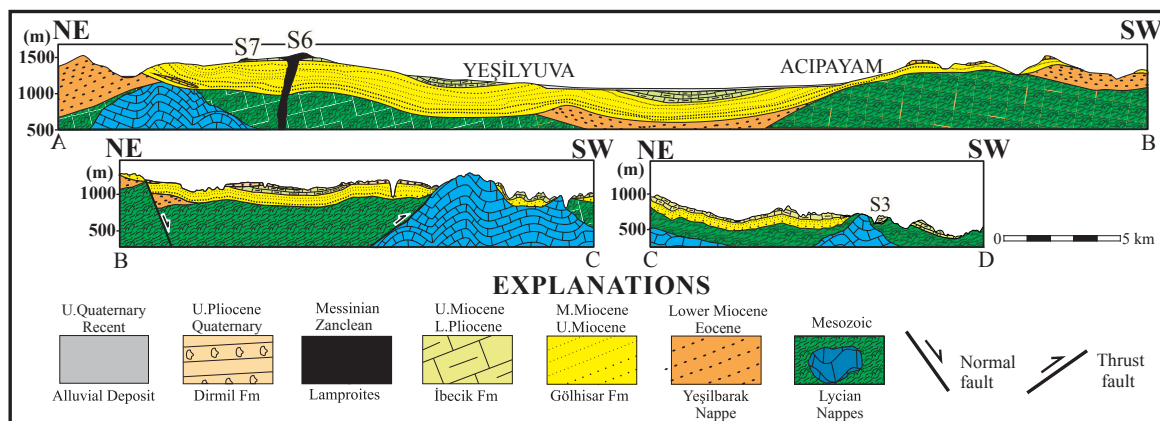


Figure 3. Geological cross-sections and correlation of lamproites and tuff levels.

deposition from late Miocene to early Pliocene (Elitez, 2010; Elitez and Yaltrak, 2014, 2016). The İbecik Formation contains sedimentary facies reflecting a shallow, warm lake and shoreline environments, including beach and delta.

2.5. Dirmil Formation

The Dirmil Formation is made of copper-colored conglomerates, mudstones, local siltstones, and claystones. This unit was named by Elitez (2010). The unit crop outs mostly north of Altınyayla (or Dirmil) on the footwall of the Kuşdili normal fault and southwest of the Çameli Basin, on the footwall of the Asar normal fault. West of the Dalaman River and south of the Acıpayam Basin, these copper-colored rocks are clearly exposed on high-elevation plains (Figure 2). The Dirmil Formation unconformably rests on the folded and tilted Göhlisar and İbecik formations. This fault-controlled deposition is observed primarily in front of the basement rocks (Figure 2). The conglomerates of the unit are poorly sorted and consist of angular to subangular pebbles supported by a matrix of mud. The total thickness of the Dirmil Formation is ~250 m. Based on its stratigraphic position and micromammal fossils (e.g., *Miomys pliocaenicus*, *Apodemus dominans*, and *Miomys praeminutus*; Erten, 2002), a late Pliocene-early Quaternary age is assigned to the formation (Elitez and Yaltrak, 2016). The sediments of the unit indicate an alluvial fan depositional environment.

3. Sampling and methods

Six lamproites and one tuff sample were collected from the study area. Lamproites cut both the İbecik and the Göhlisar formations, but we only observed intercalating lamproite levels in the İbecik Formation (Figures 2 and 3), indicating the synchronous nature of the volcanism with the İbecik Formation. Samples 4, 5, 6, 8, and 9 cut or cover the İbecik Formation (Figures 2, 3, 4a, and 4b). One lamproite sample cutting the Göhlisar Formation

was collected (i.e. S7; Figures 2 and 4c). A tuff level was collected from the İbecik Formation (i.e. S3; Figures 2, 4d, and 4e).

In the region, lamproite samples are generally mildly to highly altered. Therefore, we tried to collect less altered samples. However, each sample has a different degree of alteration. The tuff sample comes from the southern part of the region (Yolçatı village; Figures 2 and 3). The tuff layer is a pyroclastic fall deposit 2–12 cm thick. It is rich in idiomorphic biotite and feldspar minerals (Figure 5). This tuff layer accumulated between two marl layers. Different lithologies with different thicknesses can be observed in the road cut (Figures 4d and 4e). There are white lacustrine limestones, marls, and claystones. The tuff layer can be traced all along the road cut, indicating very extensive and continuous deposition. Both biotite and zircon were extracted from this sample for age determination.

3.1. ^{40}Ar - ^{39}Ar Dating

All samples were initially processed for geochronological analysis at the Mineral Separation Laboratory of the Eurasian Institute of Earth Sciences at İstanbul Technical University. Initially rock samples were crushed to reduce grain size, and then sieved for grain classification. The grain size between 125 and 250 μm was washed and dried at 105 $^{\circ}\text{C}$. Biotite minerals were separated repeatedly using a Frantz geomagnetic separator between 4 and 6 mA to at least 95% purity.

Samples were wrapped in Al foil and irradiated for 90 MWh at location 8B at the McMaster Nuclear Reactor at McMaster University in Hamilton, Canada, in irradiation package mc52. Standard hornblende MMhb-1 was used as a neutron fluence monitor with an assumed age of 520.4 Ma (Samson and Alexander, 1987). All samples were incrementally heated with a Coherent Innova 5 W continuous argon-ion laser until complete fusion was achieved. Samples were loaded into 3 adjacent wells of 2

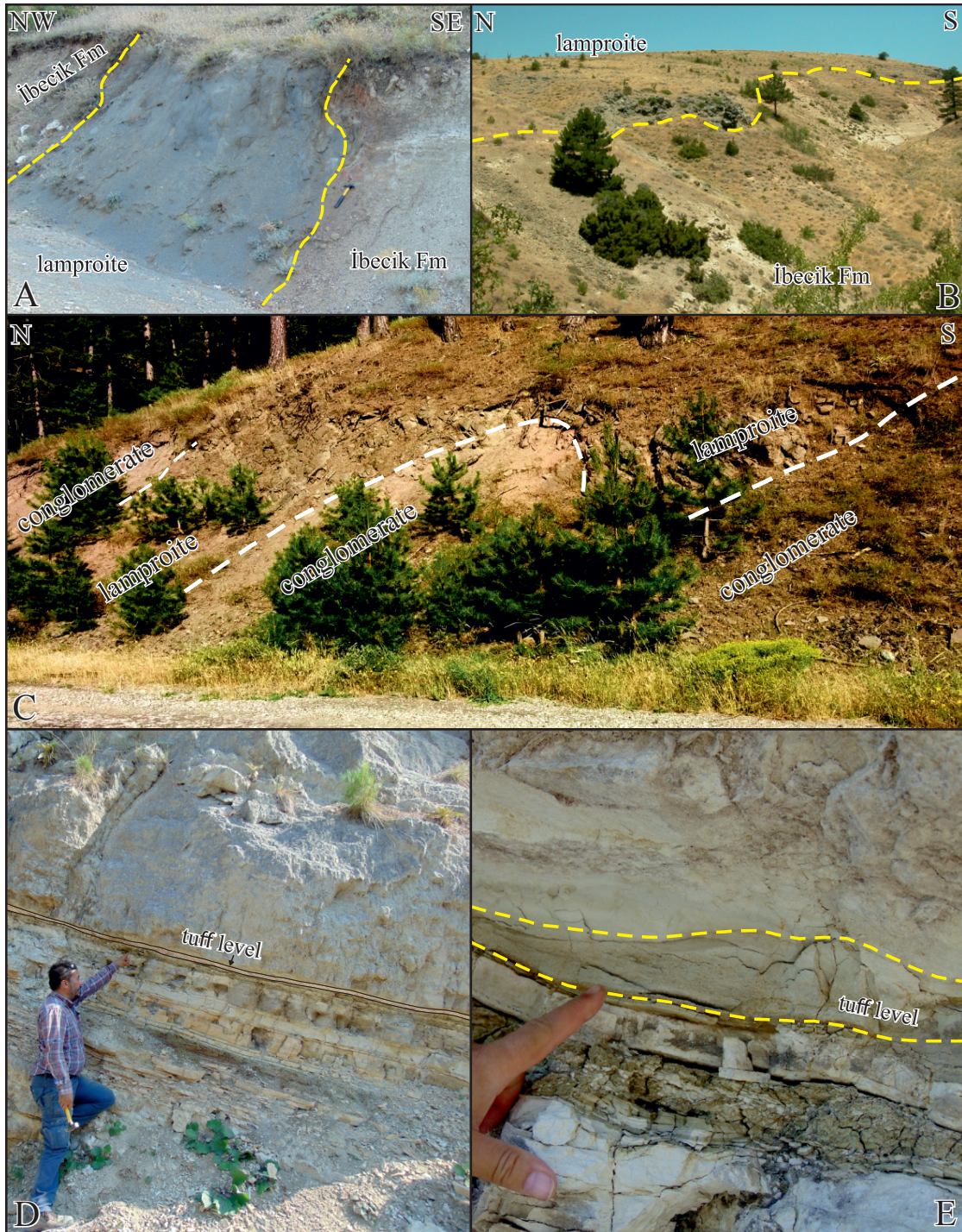


Figure 4. Examples from the outcrops of target volcanic rocks in the study area. A) Lamproite cutting the İbecik Formation (sample 5; 37°39'52.63"N, 29°22'32.92"E). B) Lamproites overlying the İbecik Formation (37°37'5.34"N, 29°21'1.38"E). C) Lamproites cutting the Gölhisar Formation (sample S7; 37°37'21.07"N, 29°28'28.45"E). D, E) Tuff level observed in the İbecik Formation (sample S3; 37°2'14.60"N, 29°4'48.29"E).

mm in diameter and each laser power setting was degassed for 30 s.

Ar isotopes were measured using a VG1200S mass spectrometer with a source operating at 150 μ A total emission and equipped with a Daly detector operating in analog mode. Mass discrimination was monitored daily using $\sim 4 \times 10^{-9}$ ccSTP of atmospheric Ar. Fusion system blanks were run every five fusion steps and blank levels from argon masses 36 through 40 ($\sim 2 \times 10^{-14}$, $\sim 3 \times 10^{-14}$, $\sim 1 \times 10^{-14}$, $\sim 3 \times 10^{-14}$, and 2×10^{-12} ccSTP, respectively) were subtracted from sample gas fractions. Corrections were also made for the decay of ^{37}Ar and ^{39}Ar , as well as interfering nucleogenic reactions from K, Ca, and Cl as well as the production of ^{36}Ar from the decay of ^{36}Cl .

3.2. Zircon U-Pb LA-ICP-MS dating

The whole-rock sample was crushed in a jaw crusher (crushing to $<0.3\text{--}0.5$ cm) and milled in a disk mill ($<0.6\text{--}1$ mm). After milling, the sample was washed and separated into heavy and light fractions, then dried. The heavy fraction was sieved and the non- to slightly magnetic fraction was separated using a magnetic separator. Heavy liquids (bromoform – 2.9 g/cm³ and methylene iodide – 3.32 g/cm³) were used to collect the zircon concentrates. The zircons were picked manually under a binocular microscope. The grains were then mounted in epoxy resin and polished. Cathodoluminescence and back-scattered images were produced at Belgrade University using a scanning SEM JSM-259 6610.

Laser ablation-inductively coupled plasma-mass spectrometry (LA-ICP-MS) analyses were carried out at the Geological Institute of the Bulgarian Academy of Science. Spatial resolution was 35 μ m and frequency was 8 Hz. The U-Pb fractionation was corrected using the GEMOC GJ-1 and raw data were processed using GLITTER4. $^{207}\text{Pb}/^{206}\text{Pb}$, $^{208}\text{Pb}/^{232}\text{Th}$, $^{206}\text{Pb}/^{238}\text{U}$, and $^{207}\text{Pb}/^{235}\text{U}$ ratios were calculated. Th disequilibrium correction was made for the results of the LA-ICP-MS. Th gets fractionated from U, imparting a disequilibrium in ^{230}Th (an intermediate product in the ^{238}U decay series) that has to be corrected to get an accurate age for younger magmatic rocks (Guillong et al., 2014). U-Pb concordia ages were calculated and plotted using ISOPLOT (Ludwig, 2003).

4. Results

Geochronological studies were carried out by two different methods to reveal the chronostratigraphy of the middle section of the Burdur-Fethiye Shear Zone. Dating results are presented in Figures 6–8, Tables 1 and 2, and the Appendix. Six lava samples and a tuff sample were dated using the $^{40}\text{Ar}/^{39}\text{Ar}$ method. An additional tuff sample was also dated by zircon U-Pb method. Eleven $^{40}\text{Ar}/^{39}\text{Ar}$ Ar dates were obtained from lamproites (samples S4–S9) located in the northern part of the study area (Figures 2,

3 and 4a–4c; Table 1). Two duplicated biotites were dated for each sample to get better results. However, the results show a wide scatter ranging from 5.83 to 12.32 Ma (Figure 6), with several ages indicating large error margins (Table 1), high MSWD values, and/or low percentages of released argon (Figure 6). Therefore, these ages were disregarded during evaluation of the chronostratigraphy of the region. Sample S4 gave two biotite ages, one of which was geologically inconsistent. Furthermore, another age had a large error range (8.23 ± 3.48 Ma; Figure 5 and Table 1). Sample S5 yielded ages of 5.06 ± 1.44 and 5.69 ± 2.34 Ma, respectively (Figure 6 and Table 1). These ages are similar considering their error margins. Sample S6 also yielded similar ages from two different biotite separates (6.08 ± 0.48 and 6.43 ± 0.29 Ma; Figure 6 and Table 1). These ages are one million years older than the ages obtained for S5. Sample S7 gave similar ages but the first age revealed a higher MSWD value and a low fraction of ^{39}Ar released (Figure 6 and Table 1). Therefore, we accepted 6.94 ± 0.35 Ma as the age of the sample. Similar to sample S7, sample S8 yielded ages around 6.9 Ma (6.98 ± 0.31 and 6.88 ± 0.22). The results of sample S9 show a plateau profile ranging between 7.92 ± 0.55 and 6.87 ± 0.38 Ma. After excluding outliers, we calculated 6.81 ± 0.30 Ma as a weighted average age for the lamproite dykes (Figure 6). We dated one sample using both $^{40}\text{Ar}/^{39}\text{Ar}$ and U-Pb LA-ICP-MS methods from a tuff layer in the İbecik Formation in the southwestern part of the study area (S3; Figures 2, 3, 4d, and 4e). This sample location consists entirely of laminated shales, marls, and limestone beds. The dated sample is a thin tuff lamina, consisting of mica, feldspar, quartz, and minor zircon ($2\text{--}3$ mm thick) intercalated with the lacustrine limestone. In the outcrop, the base contact of the tuff level is a sharp boundary (Figures 4d and 4e). This thin level is an entirely atmospheric fall-out deposit and the rest of the sequence consists of fine-grained lacustrine sediments. $^{40}\text{Ar}/^{39}\text{Ar}$ ages of sample S3 are very different from one another. The first age data are very poor and excluded. It showed a high MSWD value and low fraction of ^{39}Ar released. Another separate gave 5.83 ± 0.87 Ma. Figure 8a shows cathodoluminescence images of the zircon crystals extracted from sample S3. The zircons are perfectly idiomorphic and exhibit slight to well-expressed oscillatory zoning, typical for crystallization in magmatic conditions. The zircon grains in the sample are predominantly medium to short prismatic and some of them reveal a complex internal structure with recrystallized cores and inclusions of apatites. Thirty-one spots were analyzed and most of them yielded concordant ages (between 90% and 107%; Table 2). Some of the zircon zones yielded discordant ages, probably due to lead loss. The concordia age obtained from the zircons is 6.93 ± 0.041 Ma (Figure 8b) as crystallization age. Both zircon

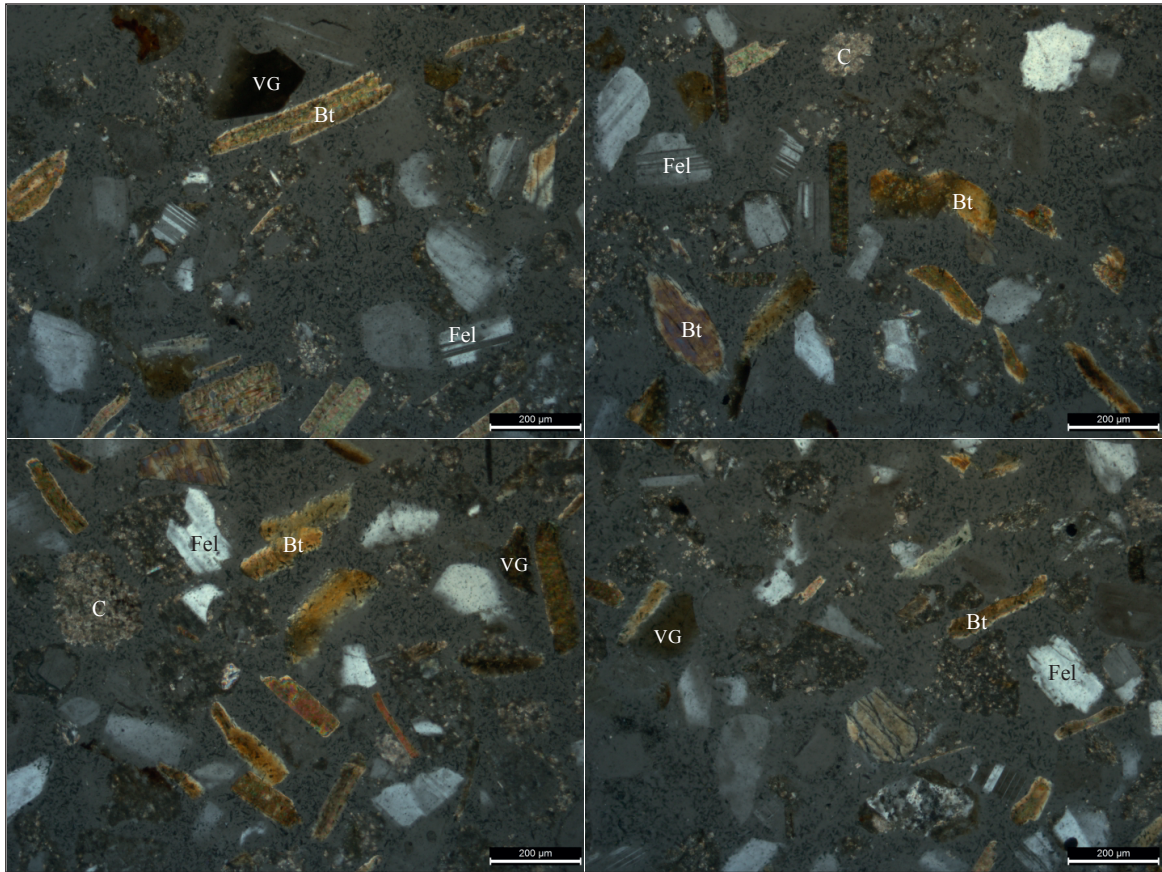


Figure 5. Photomicrograph showing mineral content of sample S3 under polarized optical microscope (Bt: biotite, VG: volcanic glass, Fel: feldspar, C: calcite).

U-Pb and biotite ^{40}Ar - ^{39}Ar r ages are identical in error ranges and correspond to a Messinian interval.

5. Discussion and conclusions

The late Miocene-Pliocene terrestrial sediments occupy wide areas on the geological maps of southwestern Anatolia (see Şenel, 1997, 2002). The timing of tectonism in this region has been determined based on limited terrestrial fossil ages (e.g., Erten, 2002; Saraç, 2003; Alçiçek et al., 2005; van den Hoek Ostende et al., 2015b). In general, the upper Pliocene carbonate sequences have not been recorded in Neogene geological history in the Mediterranean literature, except for Anatolia (e.g., Popov et al., 2006; Snel et al., 2006; Rossi et al., 2015; Guerra-Merchán, 2014; Cornée et al., 2016; Frigui et al., 2016). On the contrary, pre-Messinian and especially Tortonian carbonate environments are widespread in all Mediterranean regions (e.g., Buchbinder, 1979; Jacobs et al., 1996; Brachet et al., 1998; Krijgsman et al., 2002; Tsapas and Marcopodouluo-Dicantoni, 2005; Hüsing et al., 2009; Braga, 2016; Brandano et al., 2016; Moissette et al., 2018). The pre-Miocene sequences

and the records of the Messinian salinity crisis (Hsü et al., 1973), holding an important place in the Tertiary geology of the Mediterranean, are almost absent in southwestern Anatolia (e.g., Şenel, 1997, 2002). This situation was first noted in the northern Aegean and Marmara seas (Sakinç et al., 1999; 2000; Sakinç and Yaltrak, 2005; Snel et al., 2006), where Pliocene carbonate sequences do not exist and terrestrial conglomerates and alluvial fan sediments unconformably rest on the Miocene sequences. Based on the presence of Mediterranean fauna and the ages of cross-cutting basalts, Sakinç and Yaltrak (2005) suggested that the lower part of the limestones in the Alçiçtepe Formation (northwestern Anatolia) were deposited during the Tortonian. These authors also suggested that the upper parts of the Alçiçtepe Formation, including the brackish species, were deposited during the Messinian and that they can be considered as evidence for the inflow from the Paratethys to the Northern Aegean region during the Messinian.

The new radiometric ages provided in this study allowed a more reliable comparison between the northern Aegean

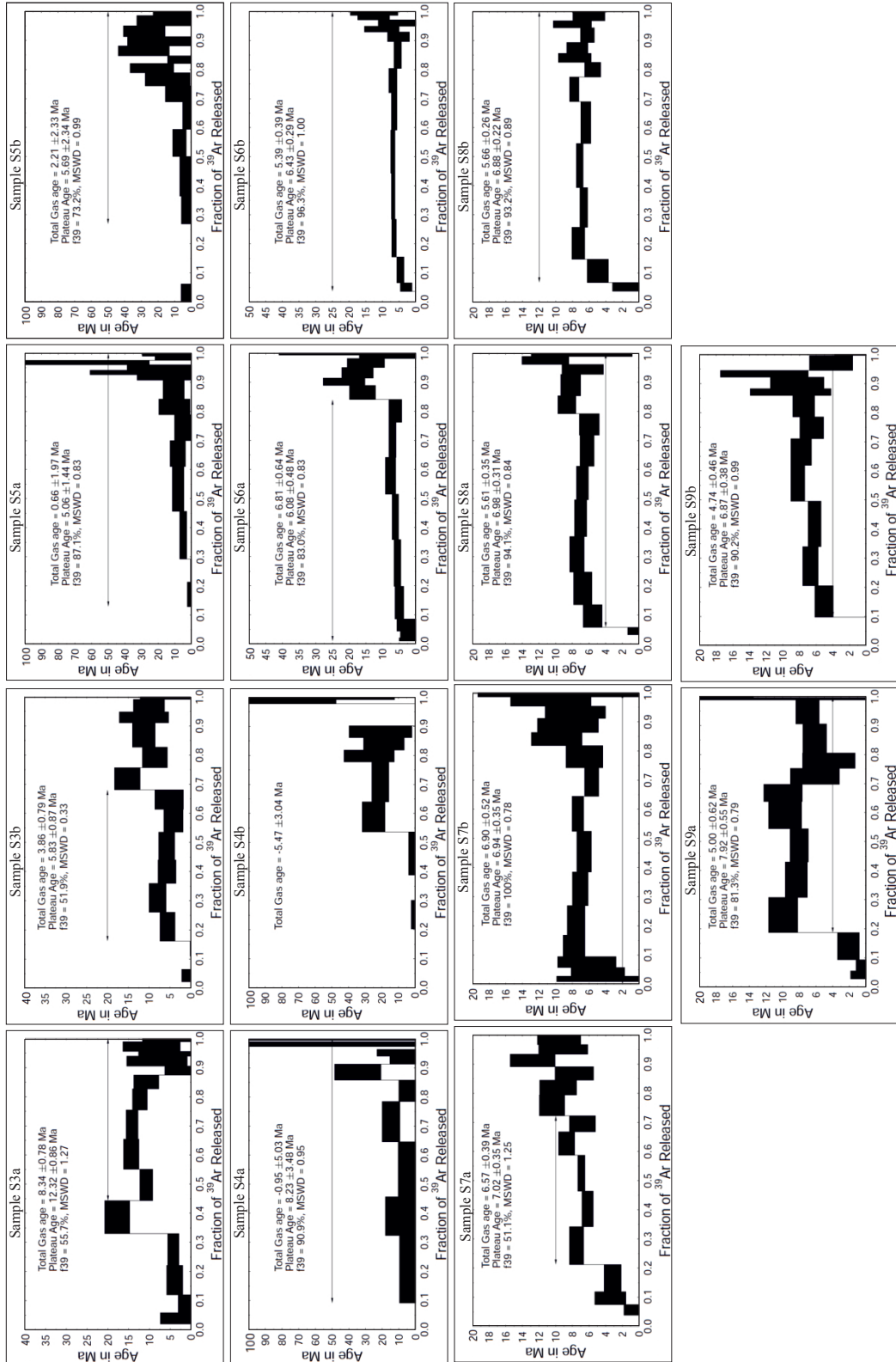


Figure 6. Diagrams of plateau ages obtained from biotites of lamproites samples. Ar isotopes were measured in the Argon Geochronology Laboratory, University of Michigan, Ann Arbor, MI, USA (analyst: Chris Hall).

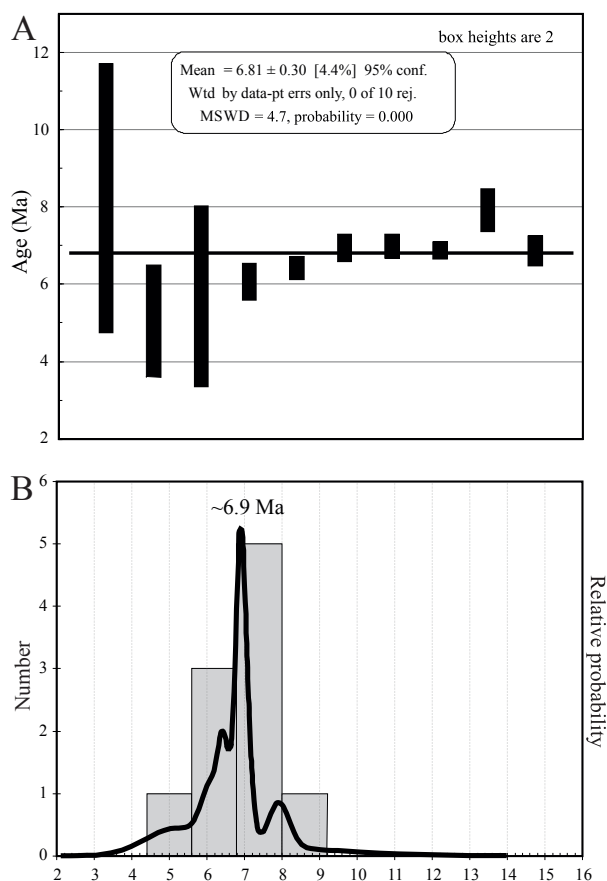


Figure 7. $^{40}\text{Ar}/^{39}\text{Ar}$ age range plots of the individual samples except tuff sample. A) Mean age calculation of the ages (Ludwig, 2003). B) Relative probability distribution of the ages.

region (i.e. northwestern Anatolia) and southwestern Anatolia. The carbonate deposition (i.e. the Alçitepe Formation) in northwestern Anatolia and the Sea of Marmara has a time-equivalent deposition in southwestern Anatolia (i.e. the İbecik Formation). Likewise, the Dirmil Formation is similar in terms of sedimentary characteristics to the late Pliocene-early Quaternary Conkbayırı Formation (Şentürk and Karaköse, 1987; Yalıtırak, 2002) in the Gelibolu Peninsula, the Samanlıdağ Formation in the Armutlu Peninsula (Alpar and Yalıtırak, 2002), and the Karacabey Formation in the Manyas Plain (Yalıtırak and Alpar, 2002). Accordingly, this sequence is time-equivalent to the Neogene sequence along the middle section of the Burdur-Fethiye Shear Zone. This left-lateral transtensional shear system created various basins. Today, these basins include the remnants of larger carbonate lakes. In previous studies, these lacustrine deposits were assigned to the Pliocene, except for the Acıpayam Basin (e.g., Şenel, 2002; Alçıçek et al., 2004, 2005, 2006, 2008; Kazancı et al., 2012). Paton (1992) dated the basaltic dykes cutting limestones

Table 1. Brief characterization of samples and their ages.

Sample	Locality	Rock	Mineral	Age, Ma
S3a*	37°2'14.60"N,	Tuff	Biotite	12.32 ± 0.86
S3b*	29°4'48.29"E			5.83 ± 0.87
S4a*	37°40'2.71"N,	Lamproite	Biotite	8.23 ± 3.48
S4b*	29°21'53.05"E			-
S5a*	37°39'52.63"N,	Lamproite	Biotite	5.06 ± 1.44
S5b*	29°22'32.92"E			5.69 ± 2.34
S6a*	37°36'12.49"N,	Lamproite	Biotite	6.08 ± 0.48
S6b*	29°27'21.85"E			6.43 ± 0.29
S7a*	37°37'21.07"N,	Lamproite	Biotite	7.02 ± 0.35
S7b*	29°28'28.45"E			6.94 ± 0.35
S8a*	37°35'18.78"N,	Lamproite	Biotite	6.98 ± 0.31
S8b*	29°26'20.69"E			6.88 ± 0.22
S9a*	37°37'2.42"N,	Lamproite	Biotite	7.92 ± 0.55
S9b*	29°27'18.40"E			6.87 ± 0.38
S3**	37°2'14.60"N,	Tuff	Zircon	6.933 ± 0.041

* $^{40}\text{Ar}/^{39}\text{Ar}$ dating; **U-Pb dating.

as upper Miocene in the north of Acıpayam Basin. This interpretation led to the separation of the same unit into two different formations (e.g., Şenel, 2002). The different age assignments for the same rocks at two different sides of the same basin created great confusion in the literature and led to misinterpretation of the geological history of the region.

Paton (1992) studied the Denizli lamproites and dated them using the $^{40}\text{Ar}/^{39}\text{Ar}$ whole-rock method with radiometric ages of 4.59 ± 0.57, 5.66 ± 0.63, 5.89 ± 0.41, 6.52 ± 0.33, 6.28 ± 0.48, and 6 ± 1.54 Ma (i.e. Tortonian-early Pliocene). At the same time, some researchers reported mammal fossils located in the south of the Acıpayam Basin and gave an age interval between 10.8 and 1.8 Ma (e.g., Saraç, 2003; Alçıçek et al., 2005; van den Hoek Ostende et al., 2015b). Elitez et al. (2016) and Elitez and Yalıtırak (2018) claimed that the geographic locations of these samples and positions of the fossils are not reliable. Therefore, stratigraphic relationships remain ambiguous. Across the northern part of the Acıpayam Basin at elevations of ~1500–1600 m, the volcanic rocks cut and/or overlie lacustrine sediments of the İbecik Formation (Figure 3). In this study, we dated biotites from seven samples of these volcanics using the $^{40}\text{Ar}-^{39}\text{Ar}$ method. However, some of the samples yielded bad results, most probably due to alteration of the samples. Furthermore, we could constrain the age range of the volcanics. The ^{40}Ar -

Table 2. Zircon LA-ICP-MS data of sample S3.

Spot	Th (ppm)	U (ppm)	Pb (ppm)	Th/U	Isotopic ratios					Apparent ages (Ma)					Concordance
					²⁰⁷ Pb/ ²⁰⁶ Pb	²⁰⁷ Pb/ ²³⁵ U	$\pm 1\sigma$	²⁰⁶ Pb/ ²³⁸ U	$\pm 1\sigma$	Rho	²⁰⁶ Pb/ ²³⁸ U	$\pm 2\sigma$	²⁰⁷ Pb/ ²³⁵ U	$\pm 2\sigma$	
1	933.13	1173.52	1.34	0.80	0.04859	0.03344	0.00685	0.00102	0.00005	0.51669	6.58	0.64	6.93	9.36	95%
2	1548.03	2579.09	2.99	0.60	0.04607	0.01395	0.00663	0.00104	0.00003	0.52244	6.72	0.39	6.71	3.99	100%
3	3174.95	3293.75	3.95	0.96	0.04298	0.01159	0.00629	0.00106	0.00004	0.53016	6.83	0.52	6.36	3.33	107%
4	2846.23	2223.47	2.93	1.28	0.04592	0.01248	0.00677	0.00107	0.00003	0.52369	6.89	0.39	6.85	3.67	101%
5	2464.87	2183.70	2.81	1.13	0.04608	0.00894	0.00680	0.00107	0.00003	0.53256	6.89	0.39	6.88	2.62	100%
6	1909.99	2053.28	2.50	0.93	0.04575	0.01430	0.00676	0.00107	0.00003	0.52041	6.90	0.39	6.84	4.19	101%
7	759.53	1219.00	1.38	0.62	0.04587	0.02033	0.00679	0.00107	0.00004	0.52002	6.91	0.52	6.87	6.00	101%
8	628.52	1058.23	1.18	0.59	0.04633	0.01482	0.00686	0.00107	0.00003	0.51995	6.91	0.39	6.94	4.33	100%
9	2898.74	2211.67	2.91	1.31	0.04571	0.00994	0.00680	0.00108	0.00003	0.52948	6.95	0.39	6.88	2.94	101%
10	1995.09	1541.33	2.09	1.29	0.04732	0.02662	0.00704	0.00108	0.00004	0.51540	6.95	0.52	7.12	7.89	98%
11*	1196.98	1229.28	1.54	0.97	0.05246	0.01510	0.00782	0.00108	0.00003	0.52215	6.96	0.39	7.91	4.47	88%
12	1655.50	1782.37	2.22	0.93	0.04627	0.01018	0.00690	0.00108	0.00003	0.52864	6.96	0.39	6.98	3.02	100%
13	1378.51	1709.69	2.03	0.81	0.04550	0.01079	0.00679	0.00108	0.00003	0.52616	6.97	0.39	6.87	3.18	101%
14*	2354.34	3038.96	3.70	0.77	0.05849	0.00871	0.00873	0.00108	0.00002	0.52804	6.97	0.26	8.82	2.58	79%
15	1863.29	2827.69	3.35	0.66	0.05135	0.01154	0.00767	0.00108	0.00003	0.52876	6.98	0.39	7.75	3.42	90%
16	1132.48	2033.75	2.29	0.56	0.04603	0.01480	0.00688	0.00217	0.00108	0.51999	6.98	0.39	6.96	4.37	100%
17	3093.72	2312.65	3.13	1.34	0.04629	0.00995	0.00695	0.00147	0.00109	0.52962	7.01	0.39	7.03	2.96	100%
18	1809.53	1496.46	2.00	1.21	0.04459	0.00979	0.00670	0.00145	0.00109	0.52783	7.02	0.39	6.78	2.92	104%
19	1436.70	1597.15	2.04	0.90	0.04588	0.01632	0.00697	0.00244	0.00110	0.52840	7.09	0.64	7.05	4.91	101%
20	1181.09	1086.60	1.43	1.09	0.04487	0.02206	0.00687	0.00333	0.00111	0.51729	7.15	0.52	6.95	6.71	103%
21*	1317.21	1329.23	1.59	0.99	0.01226	0.01416	0.00183	0.00208	0.00108	0.50813	6.96	0.52	1.85	4.21	376%
22*	7374.26	6693.73	9.19	1.10	0.09434	0.00637	0.01392	0.00090	0.00107	0.55468	6.89	0.26	14.03	1.80	49%
23*	2477.10	2162.38	2.78	1.15	0.06162	0.00969	0.00909	0.00141	0.00107	0.52700	6.89	0.26	9.18	2.84	75%
24*	3895.93	3659.24	4.80	1.06	0.08341	0.01098	0.01231	0.00156	0.00107	0.54393	6.89	0.39	12.42	3.13	56%
25*	1083.17	1900.45	2.60	0.57	0.13619	0.01353	0.02016	0.00192	0.00107	0.55619	6.92	0.39	20.26	3.82	34%
26*	834.13	954.61	1.24	0.87	0.11212	0.01787	0.01672	0.00259	0.00108	0.54866	6.97	0.52	16.83	5.17	41%
27*	2201.48	1651.83	2.57	1.33	0.13287	0.01632	0.01994	0.00235	0.00109	0.55896	7.01	0.52	20.04	4.67	35%
28*	1029.26	1121.67	1.67	0.92	0.14675	0.02497	0.02208	0.00359	0.00109	0.55246	7.03	0.64	22.17	7.12	32%
29*	1832.31	2009.34	2.66	0.91	0.09232	0.01782	0.01402	0.00262	0.00110	0.54854	7.09	0.64	14.13	5.24	50%
30*	1856.05	1951.93	2.82	0.95	0.11241	0.01223	0.01753	0.00183	0.00113	0.54906	7.29	0.39	17.64	3.65	41%
31*	1113.52	1340.18	3.74	0.83	0.36478	0.03775	0.07754	0.00697	0.00154	0.58120	9.93	1.03	75.83	13.09	13%

*Highly discordant analyses.

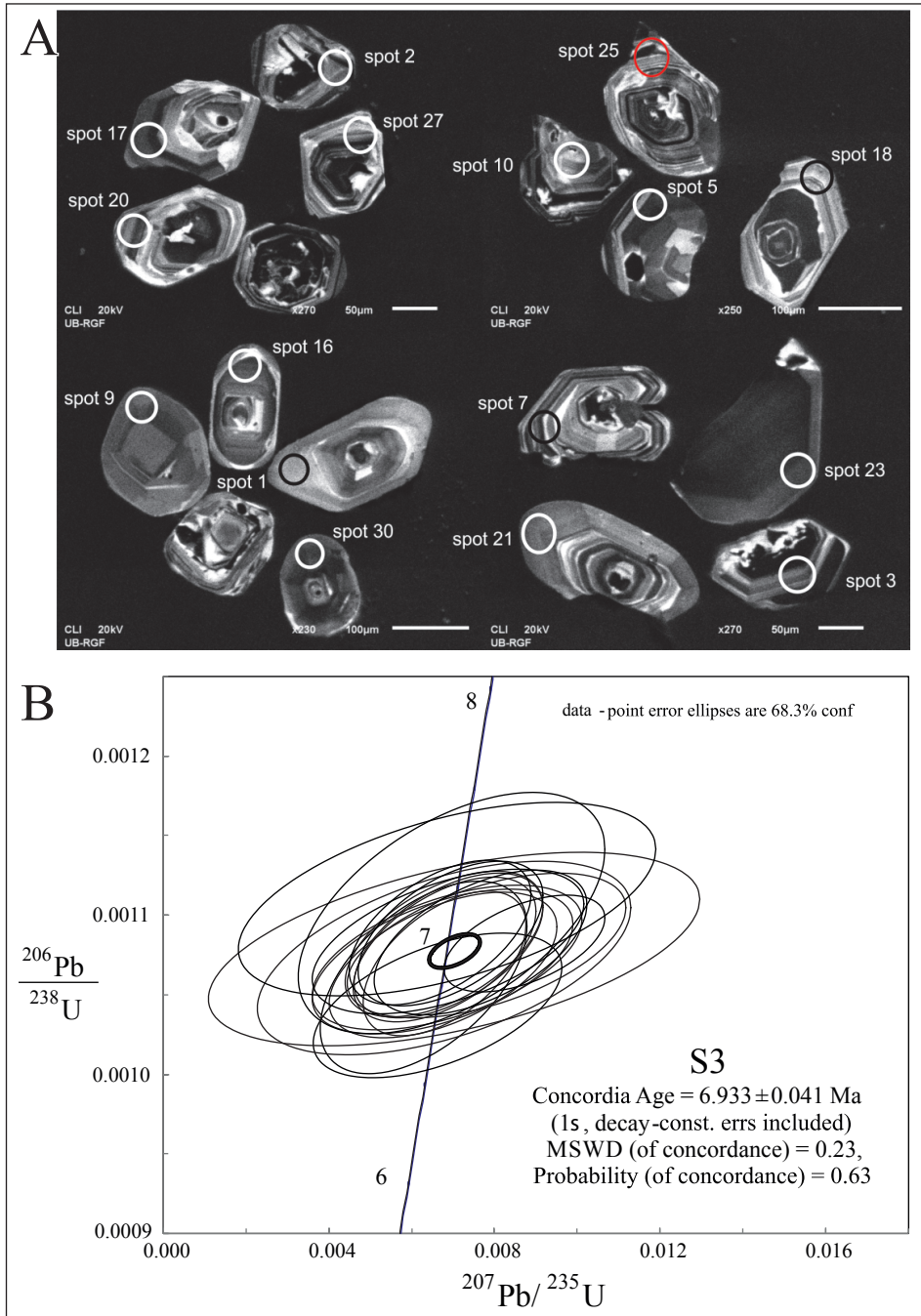


Figure 8. A) Cathodoluminescence images of zircon crystals from sample S3. B) U-Pb LA-ICP-MS data for zircons from the tuff level in the İbecik Formation.

^{39}Ar data yielded ages of 5.06 ± 1.44 , 6.08 ± 0.48 , 6.43 ± 0.29 , 6.98 ± 0.31 , 6.88 ± 0.22 , and 6.87 ± 0.38 Ma (6.81 ± 0.30 Ma weighted average; Figures 6 and 7). In addition, we obtained two important age data: 1) biotites from a lamproite dyke cutting the conglomerates of the Gölhisar Formation (Figure 4c) yielded the $^{40}\text{Ar}/^{39}\text{Ar}$ age of $6.94 \pm$

0.35 Ma, and 2) the zircon age from a tuff level intercalated with the lacustrine deposits of the İbecik Formation (Figures 4d and 4e) yielded a precise U-Pb age of 6.93 ± 0.041 Ma (Figure 7; Tables 1 and 2). The same sample also gave a 5.83 ± 0.87 Ma biotite $^{40}\text{Ar}-^{39}\text{Ar}$ age (Sample S3b; Figure 7 and Table 1).

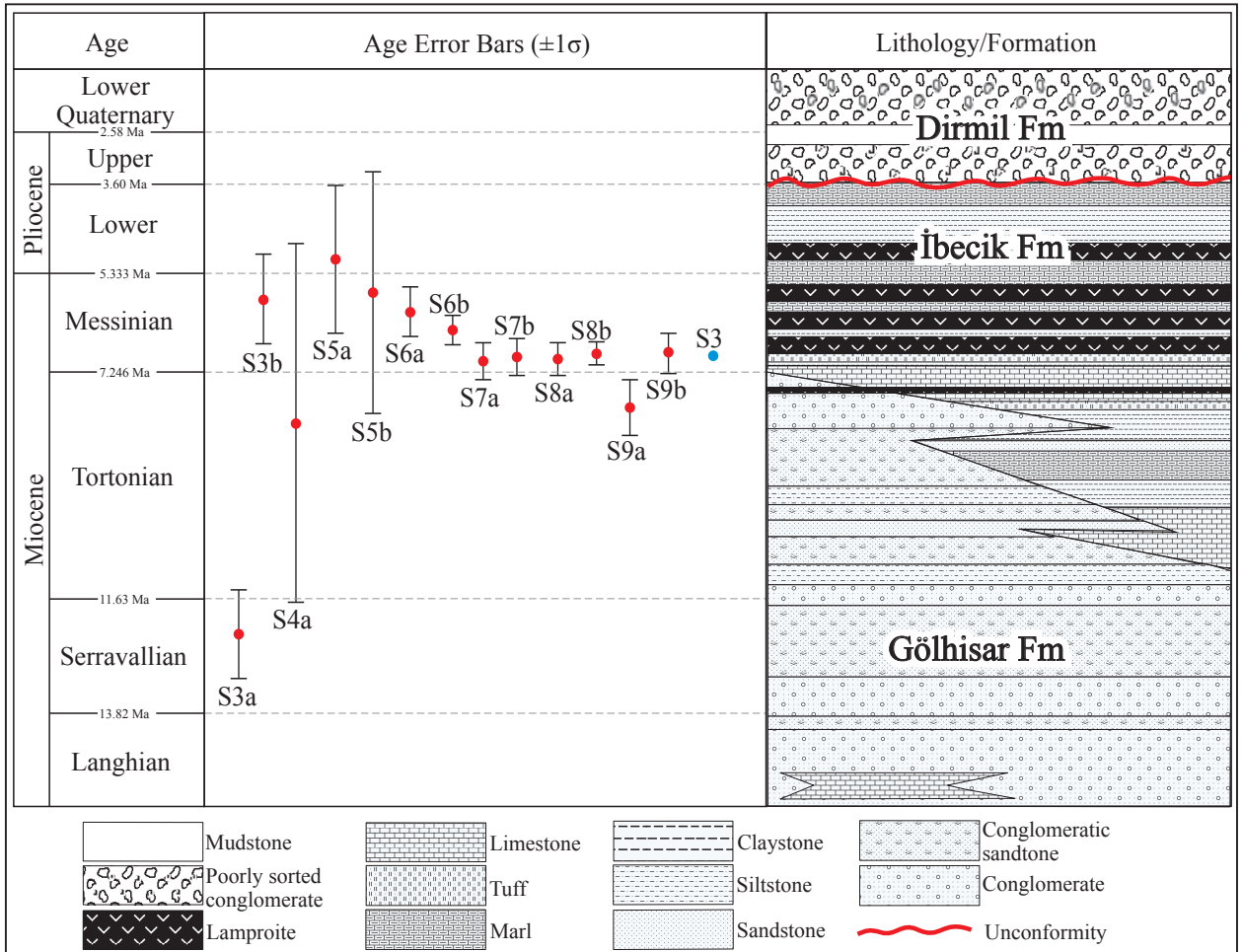


Figure 9. Generalized stratigraphic sequence of the Gölhisar, İbecik, and Dirmil formations, and age distributions of the dated samples in the sequence.

The İbecik Formation grades laterally and vertically into the Gölhisar Formation at its base. This uppermost part of the river deposits of the Gölhisar Formation indicates a lower Messinian age (Figure 9). The red wine-colored beds at the top of the İbecik Formation indicate a period of aridity, probably related to the Messinian salinity crisis, and imply intense evaporation during the Messinian (Elitez and Yaltrak, 2016). The ⁴⁰Ar/³⁹Ar and U-Pb ages demonstrated that the Burdur-Fethiye Shear Zone has been active since the middle Miocene. According to the results presented in this paper, it is well established that there was a lamproite upwelling related to the evolution of the Burdur-Fethiye Shear Zone during the Messinian. New ⁴⁰Ar/³⁹Ar and U-Pb dates unequivocally demonstrate that the lacustrine sediments located both along the northern and southern sectors of the study area are upper Miocene-lower Pliocene in age (Table 1) and that the widespread exposures of the lacustrine sediments indicate

the presence of an extensive late Miocene warm lake. This lake intensively evaporated during the Messinian salinity crisis. After the Messinian, the lake began to break up into smaller lakes associated with the evolution of the Burdur-Fethiye Shear Zone. The Acıpayam, Çameli, and Gölhisar basins were the parts of this large pre-Messinian lake.

In conclusion, the Pliocene age indicated for the lacustrine sediments in previous studies should be revised in the light of these new radiometric ages. These new ages strongly suggest that the 1.2-km-thick river facies of the Gölhisar Formation located under the lacustrine sediments of the İbecik Formation were deposited during the middle-upper Miocene. The volcanic and volcanosedimentary sequences grade laterally into the river sediments around Şuhut in the northern part of the Burdur-Fethiye Shear Zone (Figure 1). The river sediments in that region are equivalent to the sediments of the Gölhisar Formation and the ages of the volcanic

and volcanosedimentary sequences are between 15 and 8 Ma (Akal et al., 2013; Prelević et al., 2015). The decreasing radiometric ages of the volcanic rocks from north to south indicate that the Burdur-Fethiye Shear Zone is a deep tear zone between the western Anatolian extensional and the western Taurides compressional regimes since 15 Ma (Elitez et al., 2016). This study clearly documented that the lamproites in the north and the tuffs in the southernmost part of the Gölhisar-Çameli-Acıpayam basin are of the same age as the limestones in the north. Thus, the northern limestones bearing lamproite intrusions and the southern limestones including tuff layers are the same age (Figure 2 and 3). These ages indicate that the lacustrine basins on the Burdur-Fethiye Shear Zone and the timing of sedimentation are older.

The new data presented here show that the Burdur-Fethiye Shear Zone initiated during the middle Miocene in an area where there were carbonate lakes of late Tortonian-early Pliocene age. New radiometric ages are in stark contrast with the late Pliocene-early Pleistocene age for these deposits claimed by previous studies and geological maps. Finally, our results allow correlations to be established between the lacustrine sediments in

the middle part of the Burdur-Fethiye Shear Zone with sedimentary sequences of the other basins in southwestern Turkey (e.g., lacustrine sediments at ~200 m in the northern part of the Eşen Basin and at ~1200 m around Acıgöl and Burdur basins).

Acknowledgments

This study is part of the ongoing PhD studies of İrem Elitez at İstanbul Technical University. The field studies and geochronological analyses were supported by TÜBİTAK ÇAYDAG Project No. 115Y424. We thank Aral Okay (İstanbul Technical University, Turkey) for permission to use the Mineral Separation Laboratory of the Eurasian Institute of Earth Sciences at İstanbul Technical University. We are grateful to Stoyan Georgiev (Bulgarian Academy of Sciences, Bulgaria) for U-Pb dating of the volcanic rocks and Chris Hall (University of Michigan) for $^{40}\text{Ar}/^{39}\text{Ar}$ dating. We are grateful to Ali Aksu (Memorial University) and Ayberk Uyanık (Turkish Petroleum Corporation) for English editing. We thank geologists Aybars Özmen, Okan Karakoç, and Derya İpek Gültekin for their help in field and laboratory. Also, we are thankful to the reviewers and editor for helpful contributions to the manuscript.

References

- Akal C, Helvacı C, Prelević D, van den Bogaard P (2013). High-K volcanism in the Afyon region, western Turkey: from Si-oversaturated to Si-undersaturated volcanism. *Int J Earth Sci* 102: 435-453.
- Aksu AE, Hall J, Yaltrak C (2009). Miocene-Recent evolution of Anaximander Mountains and Finike Basin at the junction of Hellenic and Cyprus Arcs, eastern Mediterranean. *Mar Geol* 258: 24-47.
- Alçıçek MC, Kazancı N, Özkul M (2005). Multiple rifting pulses and sedimentation pattern in the Çameli Basin, southwestern Anatolia, Turkey. *Sediment Geol* 173: 409-431.
- Alçıçek MC, Kazancı N, Özkul M, Şen Ş (2004). Sedimentary infill and geological evolution of Çameli Neogene Basin, Denizli-SW Turkey. *Bulletin of the Mineral Research and Exploration* 128: 99-123.
- Alçıçek MC, ten Veen JH (2008). The late Early Miocene Acıpayam piggy-back basin: refining the last stages of Lycian nappe emplacement in SW Turkey. *Sediment Geol* 208: 101-113.
- Alçıçek MC, ten Veen JHT, Özkul M (2006). Neotectonic development of the Çameli Basin, southwestern Anatolia, Turkey. In: Robertson AHF, Mountrakis D, editors. *Tectonic Development of the Eastern Mediterranean Region*. London, UK: Geological Society of London, pp. 591-611.
- Alpar B, Yaltrak C (2002). Characteristic features of the North Anatolian Fault in the Eastern Marmara region and its tectonic evolution. *Mar Geol* 190: 329-350.
- Brachert TC, Betzler C, Braga JC, Martin JM (1998). Microtaphofacies of a warm-temperate carbonate ramp (uppermost Tortonian/lowermost Messinian, southern Spain). *Palaios* 13: 459-475.
- Braga JC (2016). Neogene rhodoliths in the Mediterranean basins. In: Riosmena-Rodríguez R, editor. *Rhodolith/Maërl Beds: A Global Perspective*. Berlin, Germany: Springer, pp. 169-193.
- Brandano M, Tomassetti L, Sardella R, Tinelli R (2016). Progressive deterioration of trophic conditions in a carbonate ramp environment the lithothamnion, Majella Mountain (Tortonian-Early Messinian, Central Apennines, Italy). *Palaios* 31: 125-140.
- Brunn JH, de Graciansky PC, Gutnic M, Juteau T, Lefevre R, Marcoux J, Monod O, Poisson A (1970). Structures majeures et corrélations stratigraphiques dans les Taurides occidentales. *B Soc Geol Fr* 3: 515-556 (in French).
- Buchbinder B (1979). Facies and environments of Miocene reef limestones in Israel. *J Sed Petr* 49: 1323-1344.
- Cornée JJ, Münch P, Achalhi M, Merzeraud G, Azdimousa A, Quillévéré F, Melinte-Dobrinescu M, Chaix C, Ben Moussa A, Lofi J et al. (2016). The Messinian erosional surface and early Pliocene reflooding in the Alboran Sea: new insights from the Boudinar basin, Morocco. *Sed Geol* 333: 115-129.
- Dewey JF, Şengör AMC (1979). Aegean and surrounding regions. Complex multiplate and continuum tectonics in a convergent zone. *Geol Soc Am Bull* 90: 84-92.

- Elitez İ (2010). Çameli ve Gölhisar Havzalarının Miyosen-Kuvaterner jeodinamiği, Burdur-Fethiye Fay Zonu, GB Türkiye. MSc, İstanbul Technical University, İstanbul, Turkey (in Turkish with an abstract in English).
- Elitez İ, Yaltrak C (2014). Miocene-Quaternary Geodynamics of Çameli Basin, Burdur-Fethiye Shear Zone (SW Turkey). Geological Bulletin of Turkey 57: 41-67 (in Turkish with an abstract in English).
- Elitez İ, Yaltrak C (2016). Miocene to Quaternary tectonostratigraphic evolution of the middle section of the Burdur-Fethiye Shear Zone, south-western Turkey: implications for the wide inter-plate shear zones. Tectonophysics 690: 336-354.
- Elitez İ, Yaltrak C (2018). Reply to the comment on "Miocene to Quaternary tectonostratigraphic evolution of the middle section of the Burdur-Fethiye Shear Zone, south-western Turkey: implications for the wide inter-plate shear zones". Tectonophysics 722: 601-606.
- Elitez İ, Yaltrak C, Aktuğ B (2016). Extensional and compressional regime driven left-lateral shear in southwestern Anatolia (eastern Mediterranean): the Burdur-Fethiye Shear Zone. Tectonophysics 688: 26-35.
- Elitez İ, Yaltrak C, Şahin M (2016). Vegetation and climate changes during the late Pliocene and early Pleistocene in SW Turkey -- Comment to the published paper by Jiménez-Moreno et al, Quat Res 84 (2015), 448-456. Quat Res 85: 471-475.
- Erakman B, Meşhur M, Gül MA, Alkan H, Öztaş Y, Akpınar M (1982). Toros projesine bağlı Kalkan-Köyceğiz-Çameli-Tefenni arasında kalan alanın jeolojisi ve hidrokarbon olanakları raporu. Ankara, Turkey: TPAO (in Turkish).
- Ersoy E (1990). The analysis of evolution and structural items of the western Taurus-Lycian nappes. Bulletin of the Chamber of Geological Engineering of Turkey 37: 5-16.
- Erten H (2002). Acıpayam-Çameli karasal neojen istifinin stratigrafisi ve mikromemeliler yönünden incelemesi. MSc, Pamukkale University, Denizli, Turkey (in Turkish with an abstract in English).
- Frigui M, Ben Youssef M, Ouaja M (2016) Evidences of "Lago-Mare" episode around the Messinian-Pliocene boundary in eastern Tunisia (central Mediterranean). J Afr Earth Sci 123: 57-74.
- Govers R, Wortel MJR (2005). Lithosphere tearing at STEP faults: response to edges of subduction zones. Earth Planet Sc Lett 236: 505-523.
- Göktaş F, Çakmakçoğlu A, Tarı E, Sütçü YF, Sarıkaya H (1989). Çivril-Çardak arasında jeolojisi. Ankara, Turkey: General Directorate of Mineral Research and Exploration (in Turkish).
- Graciansky PC (1972). Recherches géologiques dans le Taurus Lycien occidental. PhD, University of Paris-Sud, Orsay, France (in French).
- Guerra-Merchán A, Serrano F, Hlila R, El Kadiri K, Sanz de Galdeano C, Garcés M (2014). Tectono-sedimentary evolution of the peripheral basins of the Alboran Sea in the arc of Gibraltar during the latest Messinian-Pliocene. J Geodyn 77: 158-170.
- Guillong M, von Quadt A, Sakata S, Peycheva I., Bachmann O. (2014). LA-ICP-MS Pb-U dating of young zircons from Kos-Nisyros volcanic centre, SE Aegean arc. J Anal Atom Spectrom 29: 963-970.
- Hall J, Aksu AE, Elitez İ, Yaltrak C, Çifçi G (2014a). The Fethiye-Burdur Fault Zone: a component of upper plate extension of the subduction transform edge propagator fault linking Hellenic and Cyprus Arcs, Eastern Mediterranean. Tectonophysics 635: 80-99.
- Hall J, Aksu AE, King H, Gogacs A, Yaltrak C, Çifçi G (2014b). Miocene-Recent evolution of the western Antalya Basin and its linkage with the Isparta Angle, eastern Mediterranean. Mar Geol 349: 1-23.
- Hsü KJ, Ryan WBF, Cita MB (1973). Late Miocene desiccation of the Mediterranean. Nature 242: 240-244.
- Hüsing SK, Kuiper KF, Link W, Hilgen FJ, Krijgsman W (2009). The upper Tortonian-lower Messinian at Monte dei Corvi (Northern Apennines, Italy): completing a Mediterranean reference section for the Tortonian Stage. Earth Planet Sci Lett 282: 140-157.
- Jacobs E, Wessia H, Shields G (1996). The Monterey event in the Mediterranean: a record from shelf sediments of Malta. Paleocene 11: 717-728.
- Kazancı N, Boyraz S, Özkul M, Alçiçek MC, Kadioğlu YK (2012). Late Holocene terrestrial tephra record at western Anatolia, Turkey: possible evidence of an explosive eruption outside Santorini in the eastern Mediterranean. Global Planet Change 80: 36-50.
- Krijgsman W, Blanc-Valleron MM, Flecker R, Hilgen FJ, Kouwenhoven TJ, Merle D, Orszag-Sperber F, Rouchy JM (2002). The onset of the Messinian salinity crisis in the Eastern Mediterranean (Pissouri Basin, Cyprus). Earth Planet Sc Lett 194: 299-310.
- Le Pichon X, Angelier J (1979). The Hellenic Arc and trench system: a key to the evolution of the eastern Mediterranean area. Tectonophysics 60: 1-42.
- Ludwig KR (2003). User's Manual for Isoplot 3.00. A Geochronological Toolkit for Microsoft Excel. Berkeley, CA, USA: Berkeley Geochronology Center.
- Martín JM, Braga JC, Aguirre J, Puga-Bernabéu A (2009). History and evolution of the North-Betic Strait (Prebetic Zone, Betic Cordillera): a narrow, early Tortonian, tidal-dominated, Atlantic-Mediterranean marine passage. Sed Geol 216: 80-90.
- McKenzie D (1978). Active tectonics of the Alpine-Himalayan belt: the Aegean Sea and surrounding regions. Geophys J Int 55: 217-254.
- Meulenkamp JE, Wortel WJR, Van Wamel WA, Spakman W, Strating EH (1988). On the Hellenic Subduction Zone and the geodynamic evolution of Crete in the Late Middle Miocene. Tectonophysics 146: 203-215.
- Moissette P, Cornée JJ, Antonarakou A, Kontakiotis G, Drinia H, Koskeridou E, Tsourou T, Agiadi K, Karakitsios V (2018). Palaeoenvironmental changes at the Tortonian/Messinian boundary: a deep-sea sedimentary record of the eastern Mediterranean Sea. Palaeogeogr Palaeoclimatol 505: 217-233.

- Önalan M (1979). Elmalı-Kaş (Antalya) arasındaki bölgenin jeolojisi. PhD, İstanbul University, İstanbul, Turkey (in Turkish).
- Paton S (1992). The relationship between extension and volcanism in western Turkey, the Aegean Sea and central Greece. PhD, Cambridge University, Cambridge, UK.
- Popov SV, Shcherba IG, Ilyina LB, Nevesskaya LA, Paramonova NP, Khondkarian SO, Magyar I (2006). Late Miocene to Pliocene palaeogeography of the Paratethys and its relation to the Mediterranean. *Palaeogeogr Palaeoclimatol* 238: 91-106.
- Prelević D, Akal C, Romer RL, Mertz-Kraus R, Helvacı C (2015). Magmatic response to slab tearing: constraints from the Afyon Alkaline Volcanic Complex, Western Turkey. *J Petrol* 2015: 1-36.
- Rossi M, Minervini M, Ghielmi M, Rogledi S (2015). Messinian and Pliocene erosional surfaces in the Po Plain-Adriatic Basin: insights from allostratigraphy and sequence stratigraphy in assessing play concepts related to accommodation and gateway turnarounds in tectonically active margins. *Mar Petr Geol* 66: 192-216.
- Sakıncı M, Yaltrak C (2005). Messinian crisis: What happened around the northeastern Aegean? *Mar Geol* 221: 423-436.
- Sakıncı M, Yaltrak C, Oktay FY (1999). Palaeogeographical evolution of the Thrace Neogene Basin and the Tethian-Paratethian relations at northwest Turkey (Thrace). *Palaeogeogr Palaeoclimatol* 153: 17-40.
- Sakıncı M, Yaltrak C, Oktay FY (2000). Messinian palaeogeography and Messinian crises effect of the North Aegean Sea. In: Uysal Z, Salihoğlu I, editors. National Marine Science Conference Proceedings, pp. 208-213.
- Samson SD, Alexander EC (1987). Calibration of the interlaboratory $^{40}\text{Ar}/^{39}\text{Ar}$ dating standard, Mmhb-1. *Chemical Geology Isotope Geoscience Section* 66: 27-34.
- Saraç G (2003). Türkiye omurgalı fosil yatakları. Ankara, Turkey: General Directorate of Mineral Research and Exploration (in Turkish).
- Şenel M (1997). Geological Map of Denizli, J9 Quadrangle, No: 16, in 1:100.000 Scale Sheet. Ankara, Turkey: General Directorate of Mineral Research and Exploration.
- Şenel M (2002). Geological Map of Turkey, Denizli 1:500.000 Scale Sheet. Ankara, Turkey: General Directorate of Mineral Research and Exploration.
- Şengör AMC (1979). The North Anatolian Transform Fault: its age, offset and tectonic significance. *Geol Soc Sp* 136: 269-282.
- Şengör AMC, Görür N, Şaroğlu F (1985). Strike-slip faulting and related basin formation in zones of tectonic escape: Turkey as a case. *Soc Econ Pa* 37: 227-264.
- Şentürk K, Karaköse C (1987). Çanakkale Boğazı ve dolayının jeolojisi. Ankara, Turkey: MTA Report No. 8130 (in Turkish).
- Snel E, Mărunţeanu M, Meulenkaamp JE (2006). Calcareous nannofossil biostratigraphy and magnetostratigraphy of the Upper Miocene and Lower Pliocene of the Northern Aegean (Orphanic Gulf-Strimon Basin areas), Greece. *Palaeogeogr Palaeoclimatol* 238: 125-150.
- Tsaparas, N, Marcopodoulou-Dicantoni A (2005). Tortonian Scleractinian Corals from the island of Gavdos (South Greece). *Revue de Paléobiologie* 24: 629-637
- Tur H, Yaltrak C, Elitez İ, Sarıkavak KT (2015). Pliocene-Quaternary tectonic evolution of the Gulf of Gökova, southwest Turkey. *Tectonophysics* 638: 158-176.
- van den Hoek Ostende LW, Diepenveen E, Tesakov A, Saraç G, Mayhew D, Alçiçek MC (2015a). On the brink: micromammals from the latest Villanyian from Bıçakçı (Anatolia). *Geol J* 50: 230-245.
- van den Hoek Ostende LW, Gardner JD, van Bennekom L, Alçiçek MC, Murray A, Wesselingh FP, Alçiçek H, Tesakov A (2015b). Ericek, a new Pliocene vertebrate locality in the Çameli Basin (southwestern Anatolia, Turkey). *Paleobiodivers Paleoenviron* 95: 305-320.
- Yaltrak C (2002). Tectonic evolution of the Marmara Sea and its surroundings. *Mar Geol* 190: 493-529.
- Yaltrak C, Alpar B (2002). Evolution of the Middle Strand of North Anatolian Fault and Shallow Seismic Investigation of the Southeastern Marmara Sea (Gemlik Bay). *Mar Geol* 190: 307-328.
- Yılmaz Y, Genç SC, Gürer OF, Bozcu M, Yılmaz K, Karacık Z, Altunkaynak Ş, Elmas A (2000). When did the western Anatolian grabens begin to develop? *Geol Soc Sp* 173: 353-384.

Appendix. The measured Ar gas fractions released by laser-step heating for each of the 5 Ar isotopes in units of 1×10^{-13} ccSTP. Also included are the “J” factors and calculated ages. Measured volumes have been corrected for K, Ca AND Cl interference. All errors ARE ± 1 sigma.

Sample S3a													
Mass = 1		J = 0.00248795 \pm 0.0000173571				Tot. gas. age = 8/337 \pm 0.777							
Fraction ³⁹ Ar released	LP (mW)	Vol36	Err36	Vol37	Err37	Vol38	Err38	Vol39	Err39	Vol40	Err40	Age (Ma)	AgeErr
0.02025	100	0.02842	0.00159	0.10052	0.00681	0.09193	0.00316	0.24300	0.00259	6.36919	0.04684	-37.890	8.908
0.05817	200	0.04155	0.00146	0.10462	0.00473	0.12313	0.00268	0.45502	0.00286	12.59601	0.00978	3.146	4.263
0.11972	300	0.05718	0.00108	0.16099	0.00548	0.17260	0.00196	0.73858	0.00526	17.07755	0.02187	1.107	1.942
0.22140	400	0.06735	0.00179	0.25043	0.01100	0.26836	0.00424	1.22016	0.00592	20.96459	0.02116	3.906	1.941
0.32971	600	0.05200	0.00132	0.27981	0.00706	0.26373	0.00306	1.29961	0.00419	16.60624	0.02011	4.274	1.343
0.44346	800	0.03374	0.00285	0.24544	0.00549	0.26749	0.00263	1.36502	0.00627	15.40010	0.38362	17.769	3.012
0.55109	1000	0.03199	0.00151	0.28796	0.00576	0.24860	0.00190	1.29154	0.00516	12.56504	0.03725	10.779	1.550
0.65461	1200	0.02279	0.00175	0.29086	0.00495	0.23436	0.00240	1.24221	0.00548	10.72605	0.01647	14.371	1.854
0.75473	1400	0.01641	0.00129	0.26183	0.00786	0.22148	0.00297	1.20140	0.00515	8.66212	0.01438	14.187	1.421
0.82701	1600	0.01106	0.00116	0.27352	0.00475	0.16756	0.00355	0.86733	0.00516	5.66096	0.01736	12.347	1.765
0.87461	1800	0.00781	0.00129	0.23938	0.00929	0.11195	0.00218	0.57113	0.00394	3.68310	0.00990	10.782	2.988
0.90550	2000	0.00706	0.00142	0.21434	0.00750	0.10273	0.00230	0.37068	0.00360	2.19168	0.00935	1.275	5.072
0.93867	2400	0.00621	0.00219	0.15730	0.00697	0.08544	0.00154	0.39807	0.00455	2.56304	0.00835	8.183	7.266
0.95568	2800	0.00393	0.00154	0.08731	0.00785	0.04526	0.00108	0.20404	0.00300	1.28093	0.00869	2.637	10.020
0.98886	3200	0.00482	0.00207	0.08091	0.00586	0.07412	0.00156	0.39815	0.00406	2.26753	0.01084	9.492	6.868
1.00000	4000	0.00396	0.00234	0.06579	0.00620	0.02592	0.00147	0.13369	0.00222	0.82271	0.00662	-11.657	23.362

Appendix. (Contunied).

Sample S3b													
Mass = 1		J = 0.00248795 \pm 0.0000173571				Tot. gas. age = 3.859 \pm 0.786							
Fraction ³⁹ Ar released	LP (mW)	Vol36	Err36	Vol37	Err37	Vol38	Err38	Vol39	Err39	Vol40	Err40	Age (Ma)	AgeErr
0.02173	100	0.03266	0.00172	0.16236	0.00778	0.10198	0.00370	0.26276	0.00731	3.79217	0.05952	-102.962	9.713
0.06521	200	0.03320	0.00193	0.17192	0.00670	0.13791	0.00311	0.52583	0.00799	9.49052	0.02141	-2.726	4.886
0.11013	300	0.02749	0.00161	0.14973	0.00695	0.12304	0.00346	0.54317	0.00453	7.55646	0.02283	-4.698	3.946
0.16175	400	0.02529	0.00180	0.14221	0.00430	0.14006	0.00301	0.62414	0.00629	6.96282	0.01483	-3.666	3.832
0.26078	600	0.03487	0.00162	0.24053	0.00554	0.25432	0.00427	1.19753	0.00559	11.79238	0.04327	5.572	1.796
0.35941	800	0.03088	0.00183	0.24613	0.00802	0.23787	0.00389	1.19268	0.00689	11.23947	0.01622	7.940	2.032
0.43979	1000	0.02071	0.00159	0.19211	0.00481	0.18766	0.00367	0.97187	0.00876	7.35037	0.01917	5.674	2.168
0.53614	1200	0.02295	0.00168	0.24099	0.00979	0.22902	0.00317	1.16508	0.00601	8.27714	0.01591	5.753	1.907
0.61355	1400	0.01670	0.00162	0.20414	0.00828	0.18411	0.00353	0.93613	0.00519	5.80183	0.01741	4.152	2.291
0.68072	1600	0.01256	0.00209	0.16093	0.00661	0.15700	0.00363	0.81219	0.00629	4.65461	0.01928	5.212	3.411
0.75634	1800	0.00762	0.00213	0.23933	0.00663	0.16890	0.00245	0.91444	0.00431	5.36612	0.01232	15.226	3.061
0.82733	2000	0.01029	0.00194	0.25457	0.00492	0.17120	0.00210	0.85842	0.00647	4.69518	0.01207	8.629	2.977
0.91023	2400	0.00680	0.00205	0.32422	0.00652	0.20293	0.00306	1.00251	0.00563	4.53599	0.02036	11.276	2.696
0.94792	2800	0.00259	0.00205	0.20344	0.00627	0.09469	0.00190	0.45573	0.00495	1.90643	0.01107	11.211	5.935
0.99119	3200	0.00227	0.00148	0.18228	0.00485	0.10021	0.00230	0.52320	0.00300	1.84692	0.01350	10.056	3.726
1.00000	4000	0.00188	0.00129	0.03854	0.00500	0.02195	0.00169	0.10654	0.00338	0.46366	0.01040	-3.867	16.062

Appendix. (Continued).

Sample S4a													
Mass = 1		J = 0.00248894 ± 0.0000172331				Tot. gas. age = -0.946 ± 5.34							
Fraction ³⁹ Ar released	LP (mW)	Vol36	Err36	Vol37	Err37	Vol38	Err38	Vol39	Err39	Vol40	Err40	Age (Ma)	AgeErr
0.09114	100	0.00759	0.00219	0.04828	0.00475	0.02527	0.00172	0.15718	0.00428	0.79967	0.00952	-41.665	18.933
0.19220	200	0.00639	0.00164	0.03792	0.00603	0.01476	0.00199	0.17430	0.00289	1.77666	0.00922	-2.887	12.540
0.32345	300	0.01467	0.00190	0.02892	0.00619	0.01440	0.00156	0.22636	0.00338	4.26287	0.01288	-1.455	11.125
0.45677	400	0.01566	0.00202	0.04044	0.00617	0.01720	0.00181	0.22992	0.00435	4.95954	0.01335	6.466	11.604
0.64593	600	0.02126	0.00238	0.06343	0.00745	0.02320	0.00153	0.32624	0.00420	6.33433	0.01059	0.701	9.660
0.78398	800	0.01289	0.00096	0.05314	0.00739	0.01629	0.00212	0.23811	0.00397	4.59308	0.01275	14.720	5.307
0.85758	1000	0.00637	0.00106	0.09343	0.00806	0.01022	0.00196	0.12693	0.00338	1.85274	0.01454	-1.067	11.068
0.91240	1200	0.00180	0.00101	0.08292	0.00678	0.01033	0.00175	0.09455	0.00327	1.26738	0.00846	34.631	13.918
0.93978	1400	0.00319	0.00148	0.04453	0.00661	0.00571	0.00147	0.04721	0.00373	0.66046	0.00777	-26.965	42.373
0.96300	1600	0.00213	0.00132	0.03252	0.00659	0.00567	0.00147	0.04006	0.00321	0.44219	0.01042	-21.111	44.245
0.97303	1800	0.00198	0.00127	0.03239	0.00409	-0.00209	0.00146	0.01729	0.00267	0.16530	0.00995	-112.170	105.607
0.98489	2000	-0.00010	0.00162	0.05031	0.00730	0.00136	0.00122	0.02045	0.00163	0.14003	0.00809	36.868	103.012
0.98645	2400	0.00278	0.00138	0.01584	0.00496	-0.00173	0.00127	0.00270	0.00211	0.09018	0.00627	-1978.395	3576.32
0.98995	2800	-0.00024	0.00140	0.01144	0.00310	-0.00048	0.00096	0.00603	0.00209	0.09064	0.00753	115.844	290.589
0.99385	3200	-0.00224	0.00157	-0.00327	0.00568	-0.00162	0.00208	0.00672	0.00304	0.05269	0.00717	424.259	298.444
1.00000	4000	0.00054	0.00210	0.02384	0.00739	-0.00018	0.00206	0.01061	0.00328	0.12257	0.00647	-16.107	264.884

Appendix. (Continued).

Sample S4b													
Mass = 1		J = 0.00248894 ± 0.0000172331				Tot. gas. age = -5.47 ± 3.038							
Fraction ³⁹ Ar released	LP (mW)	Vol36	Err36	Vol37	Err37	Vol38	Err38	Vol39	Err39	Vol40	Err40	Age (Ma)	AgeErr
0.06800	100	0.01353	0.00256	0.09157	0.00666	0.06111	0.00263	0.22330	0.00339	1.73803	0.01794	-46.013	15.643
0.20278	200	0.01997	0.00158	0.11823	0.00604	0.05842	0.00275	0.44258	0.00552	3.17033	0.01165	-27.909	4.839
0.30200	300	0.03719	0.00184	0.05873	0.00648	0.03725	0.00162	0.32584	0.00249	10.60892	0.01809	-5.248	7.523
0.38828	400	0.03237	0.00188	0.05745	0.00522	0.03187	0.00165	0.28332	0.00347	8.75266	0.00976	-12.937	8.878
0.53688	600	0.04616	0.00184	0.09359	0.00799	0.04277	0.00174	0.48798	0.00506	13.50567	0.01822	-1.231	5.018
0.63961	800	0.02702	0.00177	0.06628	0.00464	0.01845	0.00206	0.33735	0.00556	9.86915	0.02506	24.913	6.897
0.77717	1000	0.03156	0.00176	0.16539	0.00585	0.02627	0.00209	0.45173	0.00487	11.43020	0.01698	20.800	5.110
0.81880	1200	0.00906	0.00158	0.15889	0.00385	0.01635	0.00213	0.13669	0.00430	3.52496	0.01256	27.635	15.134
0.86092	1400	0.00875	0.00129	0.07173	0.00414	0.00781	0.00193	0.13833	0.00422	3.16834	0.01196	18.775	12.260
0.90193	1600	0.00756	0.00193	0.05365	0.00404	0.00485	0.00219	0.13467	0.00380	2.85938	0.00810	20.744	18.826
0.92104	1800	0.01158	0.00257	0.04106	0.00944	0.00601	0.00220	0.06276	0.00358	1.46827	0.00924	-145.591	59.558
0.94208	2000	0.00768	0.00176	0.06695	0.00639	0.00528	0.00189	0.06906	0.00214	1.49953	0.00917	-50.780	34.773
0.96402	2400	0.00886	0.00186	0.04415	0.00724	0.00664	0.00185	0.07205	0.00335	1.19748	0.01003	-90.810	36.314
0.97733	2800	0.00633	0.00189	0.08254	0.00898	0.00408	0.00166	0.04373	0.00251	0.70892	0.00766	-123.364	61.791
0.99180	3200	-0.00095	0.00172	0.07915	0.00655	0.00075	0.00202	0.04753	0.00262	0.73516	0.00422	93.546	45.990
1.00000	4000	-0.00068	0.00170	0.07036	0.00597	0.00101	0.00192	0.02691	0.00225	0.36883	0.00824	92.507	80.184

Appendix. (Continued).

Sample S5a													
Mass = 1		J = 0.00248692 ± 0.0000174758				Tot. gas. age = 0.658 ± 1.973							
Fraction ³⁹ Ar released	LP (mW)	Vol36	Err36	Vol37	Err37	Vol38	Err38	Vol39	Err39	Vol40	Err40	Age (Ma)	AgeErr
0.04385	100	0.01841	0.00104	0.11001	0.00728	0.05717	0.00186	0.24656	0.00430	2.17042	0.02569	-60.481	5.919
0.12928	200	0.02144	0.00169	0.09825	0.00867	0.03828	0.00253	0.48038	0.00413	4.30591	0.02578	-19.062	4.727
0.21384	300	0.03953	0.00246	0.06926	0.00771	0.03225	0.00269	0.47545	0.00379	11.21024	0.03061	-4.459	6.880
0.29282	400	0.04427	0.00165	0.06136	0.01139	0.03114	0.00211	0.44409	0.00158	12.65572	0.01795	-4.305	4.941
0.45667	600	0.09465	0.00148	0.17339	0.00855	0.05606	0.00203	0.92135	0.00428	29.00108	0.02086	5.022	2.125
0.61038	800	0.07586	0.00228	0.29347	0.00681	0.04458	0.00211	0.86429	0.00794	23.96498	0.03172	8.024	3.492
0.69961	1000	0.04024	0.00173	0.34649	0.01318	0.02565	0.00141	0.50173	0.00391	12.81227	0.02414	8.231	4.568
0.78868	1200	0.03409	0.00228	0.54066	0.01324	0.02636	0.00204	0.50086	0.00346	10.54705	0.02041	4.223	6.032
0.84277	1400	0.01779	0.00215	0.33288	0.00522	0.01687	0.00181	0.30414	0.00352	5.95274	0.01803	10.247	9.306
0.90777	1600	0.02206	0.00175	0.74540	0.01065	0.02292	0.00144	0.36546	0.00415	7.40402	0.01561	10.819	6.317
0.92595	1800	0.00501	0.00245	0.29071	0.00628	0.00766	0.00134	0.10223	0.00329	1.50555	0.00931	1.055	31.727
0.94171	2000	0.00384	0.00274	0.30733	0.00572	0.00457	0.00171	0.08862	0.00350	1.54001	0.00840	20.388	40.565
0.95997	2400	0.00479	0.00242	0.29906	0.00480	0.01003	0.00216	0.10267	0.00301	1.58970	0.00916	7.545	31.107
0.97531	2800	0.00158	0.00257	0.22488	0.00672	0.00869	0.00181	0.08623	0.00320	1.71116	0.01293	63.652	38.232
0.98986	3200	0.00515	0.00238	0.28923	0.00563	0.00479	0.00197	0.08183	0.00225	1.21398	0.00705	-17.019	38.954
1.00000	4000	0.00301	0.00153	0.10112	0.00619	0.00200	0.00145	0.05702	0.00256	0.81570	0.00664	-5.897	35.587

Appendix. (Continued).

Sample S5b													
Mass = 1		J = 0.00248692 ± 0.0000174758				Tot. gas. age = 2.21 ± 2.33							
Fraction ³⁹ Ar released	LP (mW)	Vol36	Err36	Vol37	Err37	Vol38	Err38	Vol39	Err39	Vol40	Err40	Age (Ma)	AgeErr
0.06139	100	0.00704	0.00286	0.09061	0.00450	0.04372	0.00174	0.28550	0.00541	1.62124	0.01239	-7.207	13.335
0.16449	200	0.01727	0.00116	0.07994	0.00416	0.03490	0.00175	0.47944	0.00729	3.80321	0.01920	-12.204	3.232
0.26845	300	0.02695	0.00188	0.06398	0.00451	0.02503	0.00297	0.48342	0.00431	6.74932	0.01067	-11.317	5.200
0.36378	400	0.02457	0.00197	0.06074	0.00576	0.02459	0.00119	0.44334	0.00429	7.26544	0.01826	0.040	5.901
0.50005	600	0.04401	0.00272	0.12280	0.00534	0.03092	0.00199	0.63370	0.00562	13.17008	0.01867	1.171	5.696
0.59413	800	0.02073	0.00136	0.18397	0.00663	0.02248	0.00270	0.43748	0.00442	6.82154	0.01772	7.109	4.106
0.68895	1000	0.02740	0.00210	0.41227	0.00710	0.02538	0.00194	0.44096	0.00525	7.99224	0.01491	-1.072	6.323
0.74393	1200	0.01263	0.00221	0.31471	0.00976	0.01322	0.00200	0.25566	0.00372	3.96954	0.01423	4.171	11.412
0.78826	1400	0.00825	0.00211	0.53469	0.00726	0.01273	0.00148	0.20617	0.00404	3.09435	0.01042	14.237	13.484
0.82094	1600	0.00843	0.00151	0.22004	0.00590	0.00623	0.00166	0.15195	0.00314	3.29740	0.01429	23.663	13.039
0.84638	1800	0.00974	0.00168	0.22625	0.00712	0.01114	0.00167	0.11831	0.00374	2.75835	0.01379	-4.590	18.896
0.88139	2000	0.00923	0.00190	0.29104	0.00920	0.01166	0.00144	0.16282	0.00321	3.77431	0.01082	28.585	15.220
0.91289	2400	0.00977	0.00216	0.25788	0.00892	0.00853	0.00192	0.14649	0.00358	3.50422	0.01043	18.801	19.398
0.95016	2800	0.01102	0.00166	0.23290	0.00759	0.01029	0.00174	0.17331	0.00280	4.35740	0.00835	28.282	12.488
0.98485	3200	0.01309	0.00239	0.24878	0.00815	0.01211	0.00232	0.16131	0.00301	4.34253	0.01885	13.151	19.547
1.00000	4000	0.00690	0.00226	0.17674	0.00361	0.00483	0.00180	0.07047	0.00251	1.72517	0.00997	-20.014	42.965

Appendix. (Continued).

Sample S6a													
Mass = 1		J = 0.00248239 ± 0.0000178951				Tot. gas. age = 6.811 ± 0.644							
Fraction ³⁹ Ar released	LP (mW)	Vol36	Err36	Vol37	Err37	Vol38	Err38	Vol39	Err39	Vol40	Err40	Age (Ma)	AgeErr
0.00974	100	0.01033	0.00134	0.02368	0.00386	0.01705	0.00223	0.14672	0.00415	1.67162	0.01168	-42.675	12.419
0.02098	200	0.00436	0.00144	0.00825	0.00359	0.00433	0.00294	0.16938	0.00434	1.04970	0.00908	-6.309	11.266
0.04466	300	0.00591	0.00215	0.00614	0.00427	0.00614	0.00191	0.35687	0.00495	1.48186	0.01107	-3.337	7.976
0.08593	400	0.00614	0.00194	0.00017	0.00358	0.00888	0.00183	0.62189	0.00570	2.02789	0.01328	1.533	4.118
0.19804	600	0.00991	0.00168	0.03260	0.00316	0.01744	0.00235	1.68929	0.00687	4.80708	0.01223	4.972	1.314
0.35876	800	0.00914	0.00184	0.03723	0.00715	0.02155	0.00242	2.42173	0.00876	5.70205	0.01643	5.543	1.005
0.51498	1000	0.00687	0.00171	0.05972	0.01048	0.02188	0.00183	2.35392	0.00809	5.28793	0.00952	6.189	0.959
0.64162	1200	0.00305	0.00222	0.03206	0.00433	0.01650	0.00159	1.90826	0.00798	4.14478	0.01390	7.596	1.534
0.76213	1400	0.00354	0.00140	0.04577	0.00645	0.01568	0.00221	1.81589	0.00825	3.89824	0.01119	7.018	1.020
0.84009	1600	0.00283	0.00169	0.02179	0.00454	0.00913	0.00152	1.17465	0.00644	2.44947	0.01337	6.140	1.895
0.88893	1800	-0.00384	0.00219	0.01164	0.00555	0.00422	0.00185	0.73604	0.00447	1.51402	0.00898	16.048	3.900
0.91388	2000	-0.00319	0.00179	-0.01129	0.00694	-0.00043	0.00275	0.37588	0.00383	0.87767	0.00963	21.565	6.225
0.95036	2400	-0.00293	0.00198	0.00056	0.00506	0.00521	0.00188	0.54973	0.00534	1.29324	0.01042	17.492	4.714
0.98104	2800	-0.00156	0.00197	0.00118	0.00634	-0.00071	0.00201	0.46232	0.00332	1.09860	0.00741	15.043	5.585
0.99280	3200	0.00073	0.00141	0.00265	0.00610	-0.00213	0.00276	0.17714	0.00270	0.47255	0.00765	6.490	10.481
1.00000	4000	0.00012	0.00223	0.00374	0.00633	-0.00181	0.00197	0.10850	0.00290	0.37968	0.00737	14.117	26.966

Appendix. (Continued).

Sample S6b													
Mass = 1		J = 0.00248239 ± 0.0000178951				Tot. gas. age = 5.393 ± 0.391							
Fraction ³⁹ Ar released	LP (mW)	Vol36	Err36	Vol37	Err37	Vol38	Err38	Vol39	Err39	Vol40	Err40	Age (Ma)	AgeErr
0.01024	100	0.01990	0.00226	0.07949	0.00372	0.04316	0.00296	0.29216	0.00386	2.51488	0.03195	-52.351	10.567
0.01994	200	0.01038	0.00169	0.03018	0.00562	0.01161	0.00249	0.27670	0.00540	1.96030	0.02081	-18.024	8.189
0.03689	300	0.01159	0.00253	0.02931	0.00455	0.00808	0.00251	0.48367	0.00488	2.56540	0.01649	-7.985	6.959
0.06658	400	0.01045	0.00113	0.01908	0.00307	0.00782	0.00280	0.84726	0.00475	3.63272	0.01507	2.872	1.764
0.15483	600	0.02131	0.00203	0.04165	0.00477	0.02239	0.00255	2.51795	0.00826	8.91181	0.01695	4.647	1.063
0.28470	800	0.01288	0.00190	0.09266	0.00452	0.03362	0.00254	3.70573	0.01024	9.23562	0.01359	6.551	0.676
0.44367	1000	0.01031	0.00190	0.11585	0.00391	0.04121	0.00237	4.53578	0.01337	9.93347	0.01248	6.787	0.551
0.59133	1200	0.00789	0.00196	0.13032	0.00677	0.03305	0.00234	4.21330	0.00871	8.82856	0.01868	6.893	0.613
0.72082	1400	0.01059	0.00233	0.16463	0.00425	0.03013	0.00234	3.69451	0.01161	8.48808	0.01671	6.485	0.833
0.80385	1600	0.00453	0.00217	0.06591	0.00476	0.02153	0.00253	2.36906	0.00755	5.00627	0.01372	6.918	1.206
0.89683	1800	0.00847	0.00227	0.06119	0.00778	0.02141	0.00206	2.65320	0.01125	5.72534	0.01543	5.430	1.129
0.92886	2000	0.00266	0.00228	0.01224	0.00642	0.00620	0.00233	0.91390	0.00593	1.85241	0.00684	5.219	3.287
0.94949	2400	0.00013	0.00233	0.01706	0.00599	0.00318	0.00196	0.58871	0.00557	1.38313	0.00945	10.207	5.220
0.97064	2800	0.00207	0.00261	0.01048	0.00679	0.00619	0.00152	0.60345	0.00546	1.36373	0.01037	5.575	5.708
0.98637	3200	-0.00089	0.00162	0.01225	0.00592	0.00349	0.00147	0.44872	0.00430	1.00699	0.00731	12.643	4.748
1.00000	4000	-0.00055	0.00211	0.01377	0.00487	0.00286	0.00123	0.38890	0.00359	0.92633	0.00523	12.500	7.125

Appendix. (Continued).

Sample S7a													
Mass = 1		J = 0.00248358 ± 0.0000177989				Tot. gas. age = 6.569 ± 0.385							
Fraction ³⁹ Ar released	LP (mW)	Vol36	Err36	Vol37	Err37	Vol38	Err38	Vol39	Err39	Vol40	Err40	Age (Ma)	AgeErr
0.01125	100	0.01092	0.00126	0.04225	0.00542	0.04114	0.00226	0.20583	0.00522	2.82187	0.01061	-8.824	8.139
0.03889	200	0.01080	0.00125	0.03945	0.00596	0.05523	0.00252	0.50585	0.00526	2.55703	0.01348	-5.640	3.291
0.07501	300	0.01040	0.00153	0.02260	0.00552	0.03896	0.00243	0.66087	0.00608	2.88584	0.01180	-1.269	3.075
0.11891	400	0.00821	0.00114	0.01625	0.00519	0.02846	0.00199	0.80325	0.00701	3.04435	0.00586	3.445	1.870
0.21232	600	0.01219	0.00134	0.05045	0.00620	0.04098	0.00230	1.70930	0.00551	4.81325	0.01002	3.175	1.035
0.34269	800	0.00578	0.00156	0.22288	0.00951	0.03446	0.00187	2.38552	0.00886	5.71021	0.01907	7.503	0.864
0.46367	1000	0.00658	0.00112	0.40742	0.00695	0.02933	0.00209	2.21376	0.00791	4.99859	0.01291	6.170	0.670
0.58757	1200	0.00555	0.00074	0.52504	0.00885	0.02934	0.00219	2.26708	0.00990	5.15150	0.01041	6.927	0.434
0.66793	1400	0.00236	0.00107	0.58554	0.01138	0.02007	0.00157	1.47049	0.00715	3.55455	0.01211	8.686	0.959
0.72304	1600	0.00257	0.00119	0.43110	0.00582	0.01410	0.00124	1.00852	0.00608	2.29099	0.01236	6.792	1.561
0.79389	1800	-0.00036	0.00149	0.38770	0.00790	0.01611	0.00136	1.29636	0.00540	2.92897	0.00652	10.461	1.515
0.84428	2000	0.00015	0.00155	0.34688	0.01035	0.00864	0.00103	0.92202	0.00368	2.05179	0.01322	9.734	2.212
0.89030	2400	0.00200	0.00148	0.34708	0.00913	0.01054	0.00200	0.84219	0.00533	2.05363	0.00919	7.769	2.310
0.93336	2800	-0.00090	0.00161	0.56610	0.00760	0.01269	0.00178	0.78795	0.00508	1.98713	0.00706	12.770	2.686
0.96691	3200	0.00106	0.00137	0.33978	0.00491	0.00710	0.00206	0.61376	0.00389	1.56344	0.00854	9.111	2.941
1.00000	4000	0.00033	0.00119	0.54501	0.00788	0.00580	0.00215	0.60557	0.00594	1.39968	0.00645	9.607	2.598

Appendix. (Continued).

Sample S7b													
Mass = 1		J = 0.00248358 ± 0.0000177989				Tot. gas. age = 6.895 ± 0.52							
Fraction ³⁹ Ar released	LP (mW)	Vol36	Err36	Vol37	Err37	Vol38	Err38	Vol39	Err39	Vol40	Err40	Age (Ma)	AgeErr
0.00926	100	0.01038	0.00170	0.06561	0.00900	0.05481	0.00221	0.19468	0.00474	2.15019	0.01428	-21.241	11.718
0.02729	200	0.00619	0.00179	0.03882	0.00557	0.07701	0.00277	0.37916	0.00396	2.13562	0.01228	3.628	6.255
0.05777	300	0.00591	0.00156	0.02804	0.00506	0.07608	0.00307	0.64071	0.00448	2.45246	0.01019	4.938	3.225
0.09530	400	0.00565	0.00209	0.02378	0.00538	0.04774	0.00291	0.78917	0.00601	2.77701	0.01688	6.283	3.500
0.16889	600	0.00916	0.00154	0.04443	0.00616	0.04242	0.00260	1.54736	0.00766	5.41124	0.01933	7.810	1.310
0.26990	800	0.01135	0.00171	0.10314	0.00589	0.03429	0.00260	2.12365	0.00535	6.95088	0.01550	7.575	1.064
0.38524	1000	0.01279	0.00172	0.17279	0.00535	0.03068	0.00251	2.42519	0.00683	7.61642	0.01365	7.076	0.938
0.52464	1200	0.01344	0.00192	0.49707	0.01284	0.03295	0.00192	2.93099	0.01166	8.30516	0.01200	6.613	0.865
0.64477	1400	0.01037	0.00133	0.65991	0.00875	0.02783	0.00222	2.52582	0.00890	7.21846	0.01418	7.356	0.695
0.74291	1600	0.00879	0.00133	0.93747	0.00786	0.02259	0.00187	2.06346	0.00427	5.22803	0.01155	5.705	0.850
0.81853	1800	0.00423	0.00268	0.81742	0.00608	0.01859	0.00150	1.59004	0.00777	3.58599	0.01305	6.570	2.220
0.86285	2000	0.00063	0.00216	0.51591	0.00867	0.01444	0.00196	0.93181	0.00403	2.24735	0.00706	9.888	3.047
0.91199	2400	0.00198	0.00288	0.61531	0.01229	0.01369	0.00158	1.03308	0.00582	2.56089	0.00761	8.545	3.671
0.95393	2800	0.00832	0.00242	0.66728	0.00424	0.01482	0.00141	0.88185	0.00408	3.96486	0.01086	7.643	3.616
0.98541	3200	0.00020	0.00243	0.31256	0.00722	0.01020	0.00229	0.66200	0.00454	1.62812	0.01032	10.587	4.828
1.00000	4000	0.00085	0.00280	0.15808	0.00899	0.00495	0.00254	0.30669	0.00296	0.75465	0.00825	7.344	12.027

Appendix. (Continued).

Sample S8a													
Mass = 1		J = 0.00247437 ± 0.0000183505				Tot. gas. age = 5.613 ± 0.354							
Fraction ³⁹ Ar released	LP (mW)	Vol36	Err36	Vol37	Err37	Vol38	Err38	Vol39	Err39	Vol40	Err40	Age (Ma)	AgeErr
0.00781	100	0.02574	0.00277	0.10535	0.00751	0.05699	0.00263	0.24668	0.00748	3.03087	0.02227	-84.734	15.768
0.01720	200	0.02543	0.00150	0.05493	0.00993	0.07175	0.00293	0.29697	0.00508	6.20635	0.01263	-19.782	6.761
0.03193	300	0.04577	0.00191	0.04715	0.00825	0.08604	0.00395	0.46534	0.00365	12.38070	0.02155	-11.024	5.445
0.05753	400	0.06665	0.00160	0.03904	0.00588	0.07377	0.00267	0.80880	0.00341	19.47035	0.01766	-1.247	2.607
0.13590	600	0.12690	0.00213	0.08682	0.00916	0.09318	0.00265	2.47659	0.00865	40.59625	0.03377	5.573	1.131
0.24732	800	0.10390	0.00298	0.20080	0.00668	0.07447	0.00237	3.52061	0.01305	36.03903	0.02983	6.756	1.115
0.36994	1000	0.06600	0.00256	0.18749	0.00709	0.05924	0.00240	3.87479	0.00781	25.97611	0.03072	7.443	0.868
0.49619	1200	0.05076	0.00222	0.25662	0.00473	0.05143	0.00223	3.98936	0.00480	21.26503	0.02090	6.997	0.732
0.61189	1400	0.03134	0.00199	0.42178	0.00623	0.03740	0.00205	3.65606	0.01097	14.83634	0.02225	6.794	0.715
0.71835	1600	0.03132	0.00213	0.44904	0.00556	0.03618	0.00346	3.36391	0.01047	13.96267	0.01296	6.238	0.831
0.79138	1800	0.01697	0.00209	0.37652	0.00887	0.02481	0.00178	2.30782	0.01066	8.10903	0.02122	5.978	1.190
0.85321	2000	0.00861	0.00161	0.30717	0.00523	0.02120	0.00158	1.95364	0.00814	6.34306	0.01106	8.660	1.081
0.92728	2400	0.01210	0.00212	0.41828	0.00894	0.02317	0.00206	2.34066	0.00440	7.88701	0.01817	8.206	1.188
0.96095	2800	0.00483	0.00200	0.25110	0.00828	0.01075	0.00207	1.06383	0.00431	3.03910	0.00967	6.754	2.473
0.98894	3200	0.00040	0.00190	0.19419	0.00494	0.00516	0.00293	0.88447	0.00584	2.35095	0.00675	11.234	2.811
1.00000	4000	0.00083	0.00161	0.05403	0.00417	0.00135	0.00196	0.34942	0.00387	0.78419	0.00622	6.881	6.068

Appendix. (Continued).

Sample S8b													
Mass = 1		J = 0.00247437 ± 0.0000183505				Tot. gas. age = 5.659 ± 0.256							
Fraction ³⁹ Ar released	LP (mW)	Vol36	Err36	Vol37	Err37	Vol38	Err38	Vol39	Err39	Vol40	Err40	Age (Ma)	AgeErr
0.00717	100	0.02504	0.00145	0.12848	0.00835	0.06980	0.00210	0.34563	0.00652	3.22217	0.02731	-54.762	5.824
0.01847	200	0.03577	0.00176	0.10082	0.00514	0.07187	0.00208	0.54465	0.00267	8.77567	0.02157	-14.775	4.309
0.03767	300	0.09585	0.00237	0.06283	0.00464	0.07008	0.00297	0.92558	0.00425	27.17320	0.02219	-5.561	3.391
0.06764	400	0.13053	0.00212	0.07048	0.00822	0.06818	0.00173	1.44431	0.00563	38.97860	0.04104	1.254	1.943
0.14761	600	0.22014	0.00374	0.14190	0.01033	0.09817	0.00144	3.85469	0.00790	69.33984	0.04608	4.958	1.278
0.25772	800	0.15290	0.00309	0.23168	0.00487	0.08857	0.00293	5.30706	0.01513	53.89163	0.04146	7.310	0.765
0.39393	1000	0.11340	0.00229	0.42027	0.00403	0.09038	0.00357	6.56547	0.01077	43.33723	0.03616	6.670	0.460
0.54610	1200	0.09070	0.00231	0.57351	0.01237	0.08936	0.00243	7.33496	0.01619	38.56216	0.02442	7.144	0.414
0.68940	1400	0.06832	0.00316	0.78026	0.01223	0.08218	0.00217	6.90700	0.00865	30.13114	0.03450	6.415	0.602
0.77391	1600	0.03546	0.00173	0.49788	0.01031	0.03951	0.00236	4.07318	0.01232	17.60110	0.01898	7.789	0.559
0.82515	1800	0.02051	0.00179	0.36979	0.00904	0.02931	0.00233	2.46983	0.00997	9.15164	0.01600	5.577	0.952
0.85605	2000	0.00686	0.00223	0.13949	0.00443	0.01589	0.00226	1.48931	0.00796	4.61399	0.01184	7.737	1.972
0.89287	2400	0.00770	0.00171	0.20794	0.00902	0.01910	0.00287	1.77492	0.00822	5.23426	0.00977	7.425	1.270
0.94319	2800	0.01203	0.00154	0.59010	0.00705	0.02356	0.00251	2.42525	0.00890	6.94055	0.01409	6.222	0.837
0.96764	3200	0.00342	0.00205	0.19048	0.00693	0.00962	0.00151	1.17878	0.00757	3.13803	0.00712	8.037	2.284
1.00000	4000	0.00907	0.00227	0.16855	0.00566	0.01483	0.00193	1.55958	0.00686	4.79543	0.00892	6.042	1.912

Appendix. (Continued).

Sample S9a													
Mass = 1		J = 0.00246143 ± 0.0000186481				Tot. gas. age = 5.001 ± 0.619							
Fraction ³⁹ Ar released	LP (mW)	Vol36	Err36	Vol37	Err37	Vol38	Err38	Vol39	Err39	Vol40	Err40	Age (Ma)	AgeErr
0.01055	100	0.01590	0.00231	0.10339	0.00458	0.05062	0.00164	0.17011	0.00640	1.48755	0.03255	-85.811	19.019
0.02730	200	0.01604	0.00212	0.07875	0.00340	0.05654	0.00241	0.27003	0.00352	1.73918	0.01296	-50.013	10.621
0.05465	300	0.00954	0.00171	0.03480	0.00649	0.04695	0.00145	0.44086	0.00530	2.49570	0.01578	-3.267	5.103
0.09407	400	0.01258	0.00160	0.03636	0.00586	0.04724	0.00246	0.63550	0.00593	3.41572	0.00980	-2.109	3.315
0.18659	600	0.02415	0.00150	0.05125	0.00625	0.05645	0.00150	1.49156	0.00508	7.84528	0.01629	2.106	1.315
0.30821	800	0.01275	0.00263	0.12391	0.00528	0.05386	0.00175	1.96079	0.00705	8.17777	0.00945	9.957	1.751
0.43019	1000	0.01234	0.00199	0.46618	0.00601	0.04740	0.00096	1.96657	0.00834	7.36302	0.01826	8.370	1.326
0.54421	1200	0.00771	0.00153	0.93935	0.00749	0.04108	0.00140	1.83811	0.00450	5.61167	0.01174	8.033	1.086
0.63744	1400	0.00353	0.00228	1.40348	0.00953	0.03643	0.00217	1.50294	0.00875	4.34339	0.01534	9.727	1.982
0.69712	1600	0.00177	0.00171	0.80845	0.01270	0.02639	0.00116	0.96227	0.00581	2.68915	0.01418	9.964	2.316
0.75195	1800	0.00440	0.00198	0.82498	0.00934	0.02268	0.00188	0.88393	0.00733	2.52168	0.01113	6.133	2.934
0.80526	2000	0.00474	0.00207	1.18480	0.01040	0.01436	0.00167	0.85938	0.00671	2.26812	0.01174	4.474	3.159
0.90551	2400	0.00676	0.00174	3.27346	0.01475	0.03422	0.00245	1.61621	0.00785	4.24405	0.01219	6.161	1.411
0.98735	2800	0.00304	0.00143	2.52515	0.01201	0.02052	0.00170	1.31932	0.00495	2.98673	0.00768	7.020	1.417
0.99670	3200	0.00018	0.00170	0.59908	0.01043	0.00492	0.00243	0.15080	0.00241	0.36749	0.00645	9.205	14.721
1.00000	4000	-0.00160	0.00165	0.27930	0.00770	0.00288	0.00192	0.05321	0.00294	0.17520	0.00689	53.243	39.717

Appendix. (Continued).

Sample S9b													
Mass = 1		J = 0.00246143 ± 0.0000186481				Tot. gas. age = 5.001 ± 0.619							
Fraction ³⁹ Ar released	LP (mW)	Vol36	Err36	Vol37	Err37	Vol38	Err38	Vol39	Err39	Vol40	Err40	Age (Ma)	AgeErr
0.00955	100	0.01385	0.00111	0.12735	0.01255	0.05966	0.00222	0.18903	0.00320	1.74904	0.02844	-55.910	8.022
0.02660	200	0.01647	0.00210	0.10181	0.01087	0.08471	0.00301	0.33758	0.00345	2.84931	0.02262	-26.745	8.304
0.05520	300	0.01597	0.00173	0.07850	0.01073	0.08812	0.00226	0.56621	0.00442	3.53398	0.00948	-9.314	4.025
0.09816	400	0.02169	0.00196	0.04739	0.01151	0.07978	0.00177	0.85043	0.00506	5.56622	0.00806	-4.403	3.031
0.20607	600	0.03126	0.00180	0.12227	0.01102	0.09008	0.00237	2.13628	0.00624	11.67378	0.01732	5.058	1.106
0.34004	800	0.02012	0.00188	0.55291	0.00671	0.07991	0.00323	2.65210	0.00877	9.95475	0.01153	6.698	0.925
0.49628	1000	0.01997	0.00181	1.02736	0.00982	0.08229	0.00139	3.09309	0.00880	10.23043	0.01187	6.205	0.766
0.61884	1200	0.00733	0.00153	1.49518	0.01468	0.06553	0.00243	2.42641	0.00509	6.67376	0.02052	8.228	0.825
0.71075	1400	0.00482	0.00169	1.63944	0.01146	0.03705	0.00275	1.81958	0.00862	4.63361	0.01043	7.815	1.216
0.78558	1600	0.00479	0.00159	1.76636	0.01008	0.03090	0.00210	1.48135	0.00812	3.60325	0.01083	6.545	1.408
0.85871	1800	0.00309	0.00146	2.71298	0.01359	0.02615	0.00190	1.44761	0.00657	3.36523	0.00833	7.503	1.316
0.88250	2000	0.00053	0.00175	0.68587	0.00961	0.01567	0.00246	0.47101	0.00538	1.12042	0.00682	9.074	4.847
0.92119	2400	0.00109	0.00188	2.09052	0.01465	0.01590	0.00255	0.76607	0.00485	1.75434	0.01124	8.279	3.210
0.94516	2800	-0.00073	0.00192	1.29965	0.01300	0.01211	0.00229	0.47441	0.00400	1.09573	0.00691	12.234	5.283
0.99602	3200	0.00449	0.00200	3.02462	0.01962	0.02442	0.00226	1.00685	0.00554	2.28657	0.00857	4.226	2.604
1.00000	4000	0.00151	0.00104	0.19102	0.00700	-0.00096	0.00165	0.07885	0.00333	0.20557	0.00670	-13.599	17.424